



ELSEVIER

Palaeogeography, Palaeoclimatology, Palaeoecology 151 (1999) 267–305

PALAEO

Reconstruction of the Late Miocene climate of Spain using rodent palaeocommunity successions: an application of end-member modelling

Jan A. van Dam^{a,*}, Gert Jan Weltje^{b,c}

^a Faculty of Earth Sciences, Utrecht University, Budapestlaan 4, NL-3584 CD Utrecht, Netherlands

^b Subfaculty of Applied Earth Sciences, Delft University of Technology, Mijnbouwstraat 120, NL-2628 RX Delft, Netherlands

^c Netherlands Institute of Applied Geosciences TNO, P.O. Box 157, NL-2000 AD Haarlem, Netherlands

Received 11 February 1998; accepted 30 November 1998

Abstract

End-member modelling is applied to a data set of relative abundances of 67 Upper Miocene rodent associations (11–6 Ma) from Spain, France, Austria and Greece. The analysis results in the robust estimation of relative levels of four climatic parameters: humidity, temperature, seasonality type and predictability. In the preparatory stage, species are aggregated into nine groups on the basis of ecological criteria. Humidity preferences and adaptations are based on actualistic and functional morphological interpretations of dentition and locomotion. Temperature preferences are inferred from palaeobiogeographic distributions. Levels of adaptation to seasonality type (wet–dry or cool–warm seasonality) are assigned on the basis of diversities in present-day climate/vegetation zones, and the ability of extant relatives to hibernate. Demographic data are used to formulate adaptations to climatic (un)predictability. In the modelling stage, the compositions are unmixed into the contributions of four end members. These four extreme, theoretical rodent compositions are interpreted in climatic terms, and their contributions to the samples are used for the estimation of climatic parameters. The subset of 44 well-dated rodent compositions from the Calatayud-Daroca and Teruel basins (NE Spain) is used to construct detailed climatic curves for the Late Miocene, while the geographical dimension in the data set is used to calculate inter-basinal differences. The model results for Spain indicate more humid and cooler conditions between 10.5 and 8.5 Ma, around 7, and around 6 Ma, and more arid and warmer conditions before 10.5, between 8.6 and 7.5 Ma and around 6.5 Ma. Superimposed on this pattern is a shift from a more predictable, cool–warm seasonal climate towards a more unpredictable, wet–dry seasonal climate between 9.4 and 8.2 Ma. Inter-basinal comparisons per time slice show that the climate in southern Europe was drier, warmer, more wet–dry seasonal and more unpredictable than in central Europe, and that the climatic and vegetational boundaries between the two regions were sharp. The occurrences of more humid and cooler episodes in Spain during the Late Miocene might be explained by southward migrations of the boundary between a temperate and subtropical-dry climatic belt and their associated vegetation types. Various positive correlations are observed between the rodent-based climatic curves for Spain, and other palaeoclimatic records from the Mediterranean and NE Atlantic region (clay minerals, marine fauna, stable isotopes). The two cooling maxima at 9.4 and 7 Ma closely correspond to clusters of marine events which are generally considered to reflect maxima of global ice volume. © 1999 Elsevier Science B.V. All rights reserved.

Keywords: Miocene; palaeoclimatology; palaeoecology; Rodentia; Spain; end-member modelling

* Corresponding author. Tel.: +31 30 2535178; Fax: +31 30 2537725; E-mail: jdam@geo.uu.nl

1. Introduction

The Late Miocene is generally considered to represent an important episode in the trend known as ‘Cenozoic climatic deterioration’. Although the evidence for global cooling during this period is less evident than that for the Middle Miocene and Plio–Pleistocene (Barron, 1985; Frakes et al., 1992), the Late Miocene is characterized by very marked changes in terrestrial ecosystems. Well known among these changes is the strong expansion of more open vegetation: woodlands start to replace forests, and savannas and grasslands establish themselves on a global scale (Wolfe, 1985; Potts and Behrensmeyer, 1992; Quade and Cerling, 1995). As a reaction to these changes faunal diversifications occurred, for instance in open-vegetation herbivores and large mammalian carnivores (Van Couvering, 1980; Potts and Behrensmeyer, 1992; Janis, 1993). Although the general picture is clear, little is known about how and when this Late Miocene palaeoenvironmental transition occurred in the different continents and regions. In order to study this, more long, continuous, well-documented, and dated palaeoclimatic records are needed (Badgley and Behrensmeyer, 1995).

Fossil mammal successions have been used more extensively in palaeoecology during the last few decades. The classic successions of the Palaeogene of North America and the Neogene of the Siwaliks have shown the large potential of mammal successions for terrestrial palaeoecology (Barry et al., 1990; Gunnell et al., 1995; Morgan et al., 1995). Here we focus on NE Spain, where a high-resolution time frame has been established, based on micromammal successions. This holds in particular for the Neogene sections of the Calatayud–Daroca and Teruel basins (van de Weerd, 1976; Daams et al., 1988; Mein et al., 1990; van der Meulen and Daams, 1992; van Dam, 1997). Detailed quantitative climatic reconstructions for the Early–Middle Miocene were made by van der Meulen and Daams (1992) on the basis of rodents. Magnetostratigraphic studies (Krijgsman et al., 1994b, 1996) have allowed correlations to the Geomagnetic Polarity Time Scale (GPTS). As a result, major climatic changes, e.g. the global mid-Miocene cooling event, have been accurately dated in Spain (Krijgsman et al., 1994b).

Here we will concentrate on the Upper Miocene rodent succession of the Calatayud–Daroca and Teruel basins (hereafter referred to as CT basins). We use an ecology-based grouping of rodents. Functional morphological interpretations of the dentition and locomotion are used to formulate humidity preferences. (Palaeo)biogeographic distributions are used to infer temperature preferences. Information on the demography and life-history strategies of extant rodent groups is used to model seasonality type (temperature versus humidity-related seasonality), and predictability or interannual variation (see also van Dam, 1997).

We subject relative abundance data to the multivariate approach called end-member modelling (cf. Full et al., 1981; Renner, 1993; Weltje, 1994, 1997). This multivariate technique is based on the concept of mixing. All observations are considered to be ‘mixtures’ of a limited number of extreme compositions, which in our case represent rodent assemblages assumed to be characteristic of extreme ecological conditions. Algorithms of Weltje (1994, 1997) are used to ‘unmix’ the samples into the contributions of the end members. The end-member assemblages are interpreted in terms of climate, using inferred ecological preferences. The relative contributions of each end member to the samples are used to derive values for climatic parameters at each fossil locality. Because we also include 23 compositions from other parts of Europe (France, Austria and Greece) in the analysis, the modelling results show a geographical dimension as well.

2. Material

Our data set consists of rodent compositions from 67 South and Central European Late Miocene localities (Table 1). Forty-four of these are located in the two adjacent basins of Calatayud and Teruel (CT basins), situated in the provinces of Teruel and Zaragoza, NE Spain (Fig. 1). Taxon identifications are after van de Weerd (1976), Besems and van de Weerd (1983), van der Meulen and Daams (1992), A.J. van der Meulen (data base), and van Dam (1997). The studied time slice (~11 to 6 Ma) includes the Vallesian and a large part of the Turolian, which correspond to Neogene mammal zones MN9–10 and MN11–13, respectively (Mein, 1990;

Table 1
Localities used in this study

MN zone	Locality	Code	Interpolated age (Ma)	MN zone	Locality	Code	Interpolated age (Ma)
<i>Teruel–Alfambra region, Teruel basin, Spain</i>				<i>Vallès-Penedès basin, Spain</i>			
13	Las Casiones superior	KSS	6.05	10	Trinxera Nort Autopista	TNA	
13	Las Casiones	KS	6.10	10	Trinxera Sur Autopista 2	TSA2	
13	Valdecebro 3	VDC3	6.27	9	Can Llobateres	CL	
13	Masada del Valle 7	MDV7	6.65	9	Can Ponsich	CP	
12	Concud	CC	6.83	9	Hostaletes superior	HSS	
12	Concud 3	CC3	6.88	<i>Duero basin, Spain</i>			
12	Los Mansuetos	LM	6.90	10	Torremormojon 1	TOR1	
12	Concud 2	CC2	6.92	<i>Languedoc central, France</i>			
12	Tortajada	TO	6.93	10	Montredon	MONTR	
12	Villalba Baja 2	VB2	6.95	<i>Cucuron–Basse Durance basin, France</i>			
12	Masada del Valle 5	MDV5	7.00	12	Cucuron Stade	CUCS	
12	Masada del Valle 4	MDV4	7.05	<i>Rhone basin/area, France</i>			
12	Tortajada D	TOD	7.08	13	Lissieu	LS	
12	Tortajada C	TOC	7.08	11	Ambérieu 3	AMB3	
12	Masada del Valle 3	MDV3	7.11	11	Dionnay	DION	
12	Concud B	CCB	7.12	11	Ambérieu 2	AMB2	
12	Masada del Valle 2	MDV2	7.25	11	Ambérieu 1	AMB1	
12	Los Mansuetos 2	LM2	7.32	10	Soblay	SOBL	
11	Vivero de Pinos	VIP	8.08	10	Douvre	DOUVR	
11	Tortajada A	TOA	8.10	<i>Vienna basin, Austria</i>			
11	Los Aguanaces 3	AG3	8.11	11	Eichkogel	EICHK	
11	Alfambra	ALF	8.17	<i>Rafina basin, Greece</i>			
11	Puente Minero 3	PM3	8.18	12	Pikermi 4	PK4	
11	La Gloria 10	GLO10	8.21	<i>Strimon basin, Greece</i>			
11	Los Aguanaces 1	AG1	8.26	10	Lefkon	LEF	
11	Puente Minero	PM	8.28	Ages are calibrated to the time scale of Cande and Kent (1995). Age estimates for the localities of the Teruel–Alfambra region are interpolations based on magneto-, litho- and biostratigraphy and evolutionary stages in murids in this region (Krijgsman et al., 1996; van Dam, 1997; Garcés et al., 1999), on an age estimate of 9.7 Ma for the MN9/10 boundary in the Vallès-Penedès basin (Garcés et al., 1996), on an age estimate of 7.5 Ma for the MN11/12 boundary in the Cabriel basin (Opdyke et al., 1990; reinterpretation by Krijgsman et al., 1996), and a minimum age of about 6 Ma for the locality Venta del Moro in the Cabriel basin (Opdyke et al., 1990). See van Dam (1997: appendix B) for details on age interpolations.			
11	Peralejos D	PERD	8.70	^a Age estimate for CU on the basis of molar size of <i>Occitanomys adroveri</i> (cf. van Dam, 1997, table B.3).			
10	Peralejos C	PERC	8.84	^b Age estimates for NOM, CASAL and CAR1 are based on interpolation between estimates in the Vallès-Penedès basin of 11.1 and 10.4 Ma for the MN7–8/9 and ‘MN9A/9B’ boundaries, respectively (Garcés et al., 1996). Equal temporal spacing of the three localities during early MN9 is assumed.			
10	La Roma 2	R2	8.91	^c The age difference between PED2A and PED2C is based on their stratigraphic distance (Freudenthal and Sondaar, 1964) and average sedimentation rates in the Middle Miocene of the area (from Krijgsman et al., 1994b). The two localities are placed in the middle of local zone I, which correlates to the <i>Cricetulodon</i> zone of Agustí and Moyà-Sola (1991), dated at 10.4–9.7 Ma (Garcés et al., 1996).			
10	Puente Minero 2	PM2	9.08				
10	Masía de la Roma 11	ROM11	9.16				
10	Masía del Barbo 2B	MBB	9.24				
10	Peralejos 4	PER4	9.30				
10	Masía de la Roma 9	ROM9	9.36				
10	Masía del Barbo 2A	MBA	9.37				
10	Masía de la Roma 7	ROM7	9.41				
10	Masía de la Roma 4C	ROM4C	9.53				
9	Masía de la Roma 3	ROM3	9.67				
9	Peralejos 5	PER5	9.67				
<i>Teruel–Ademuz region, Teruel basin, Spain</i>							
12	Cubla	CU	7.00 ^a				
9	Casas Altas	CASAL	10.7 ^b				
<i>Daroca region, Calatayud–Daroca basin, Spain</i>							
9	Pedregueras 2C	PED2C	10.0 ^c				
9	Pedregueras 2A	PED2A	10.2 ^c				
9	Carrilanga 1	CAR1	10.5 ^b				
9	Nombrevilla	NOM	10.9 ^b				
<i>Alicante, Spain</i>							
12	Crevillente 5	CR5					
12	Crevillente 4	CR4					
11	Crevillente 3	CR3					
11	Crevillente 2	CR2					
11	Crevillente 1	CR1					

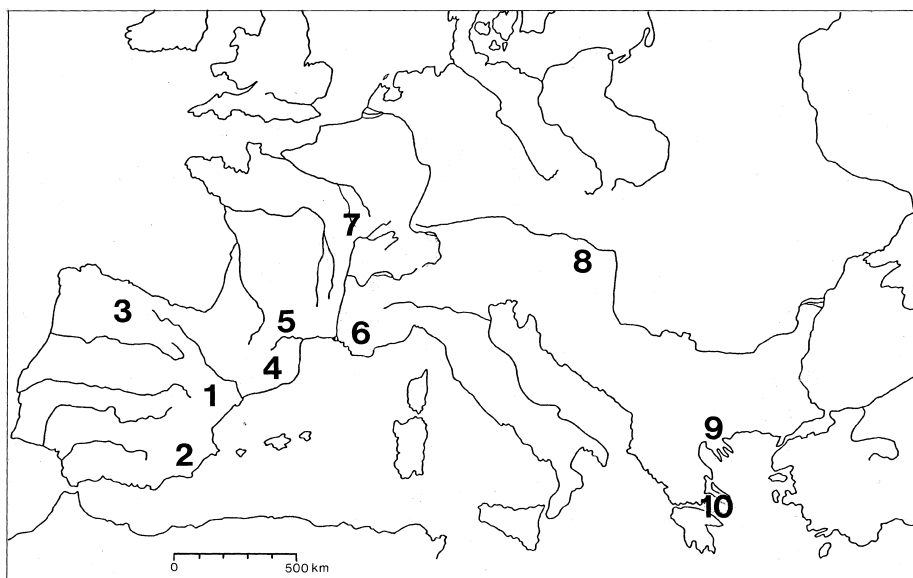


Fig. 1. Positions of the basins/areas referred to in this study: 1 = Calatayud–Daroca and Teruel; 2 = Alicante; 3 = Duero; 4 = Vallès-Penedès; 5 = Languedoc Central; 6 = Cucuron–Basse Durance; 7 = Rhone; 8 = Vienna; 9 = Strimon; 10 = Rafina.

de Bruijn et al., 1992). Numerical ages have been assigned to these localities within a framework of magneto-, litho-, and biostratigraphy (Krijgsman et al., 1996; van Dam, 1997; Garcés et al., 1999). The material is stored in the Institute of Earth Sciences of Utrecht University, the Geology Faculty of the University Complutense of Madrid, the National Natural History Museum of Leiden, and the National Museum of Natural Sciences of Madrid.

A group of 23 localities from other basins in Spain, France, Greece and Austria is included into the data set to provide a regional dimension to the analysis (Table 1; Fig. 1). Faunal information comes from Hugueney and Mein (1965), de Bruijn et al. (1975), de Bruijn (1976, 1989), Daxner-Höck (1980), Agustí (1981, 1990), Agustí and Gibert (1982a,b), Alvarez Sierra (1983), Mein (1984), Aguilar and Michaux (1990), P. Mein (pers. commun., 1995) and A.J. van der Meulen (data base). Lissieu (Lyon area, MN13) is the only karst locality in the data set. It is included because there are no other stratified northern localities of MN12–13 age for which quantitative data are available.

Relative abundances for the CT basins were based on the number of first and second molars. In case these were absent but other teeth or skeletal material was present, frequencies were counted as one. Frequen-

cies were also counted as one in case skeletal material (e.g. teeth of Castoridae) originated from a macro-mammal sample. Damaged molars were counted as one unless their surface amounted to less than half of the original surface. Differences with counts of van de Weerd (1976) are mainly due to a different treatment of damaged specimens, and the addition of some unpublished material collected by van de Weerd.

The counts for most of the other basins were also based on first and second molars. Relative abundances for Eichkogel (Austria) and most French localities were based on the available totals of first, second and third molars. The abundances for Montredon (Languedoc Central, France) were based on first and second molars for Gliridae and on first molars for the rest of the rodents.

3. End-member modelling

3.1. Palaeoecological models based on compositional data

Various types of methods and techniques can be used to model compositional variation in palaeoecological assemblages (Birks, 1985; Reyment and Jöreskog, 1993). A widely used technique for quan-

titative ecological modelling is canonical community analysis (CANOCO), a combination of correspondence analysis and canonical correlation analysis (ter Braak, 1986, 1987). This technique relates relative abundances of groups of organisms (e.g. taxa or guilds) to environmental factors, using estimates of the environmental parameters of interest at each locality. It has shown to be a useful tool in modelling of modern ecosystems. In palaeoecological studies, however, the level of detail required for successful application of this method is usually not available. The very objective of many studies, including this one, is to produce such estimates, implying that other approaches are necessary.

We use a technique known as end-member modelling (Klovan and Miesch, 1976; Miesch, 1976; Full et al., 1981, 1982; Renner, 1993; Weltje, 1994, 1997), which attempts to capture the observed variation among compositions in terms of linear mixing. Linear mixing models of compositional data summarize variation among a series of observations in terms of proportional contributions of actual or theoretical end members. In our case, the end members represent a series of faunal assemblages of extreme composition, which are assumed to reflect divergent palaeoecological conditions. The ecological setting of each individual locality is then inferred by robust interpolation on the basis of proportional end-member contributions. Because the end-members are simply compositions, they are easy to interpret by palaeontologists. This is one of the reasons we prefer this approach over methods such as correspondence analysis, where the estimated components are abstract factors requiring some a-posteriori interpretation.

3.2. The linear mixing model

Compositional data are generally cast into the form of a matrix X , with n rows representing observations (samples), and p columns representing variables. The compositional variables are non-negative, and each row of the data matrix sums to a constant c , usually 1, 100, or 10^6 (for measurements recorded as proportions, percentages, or parts per million, respectively).

$$\sum_{j=1}^p x_{ij} = c \quad x_{ij} \geq 0 \quad (1)$$

If compositional variation among a series of samples results from a mixing process, each row of the matrix of compositional data X is a non-negative linear combination of the q rows of B , a matrix of end-member compositions. The matrix M represents the proportional contributions of the end members to each observation. In matrix notation, this perfect mixing can be expressed as

$$X = MB \quad (2)$$

subject to the following non-negativity and constant-sum constraints:

$$\sum_{k=1}^q m_{ik} = 1 \quad m_{ik} \geq 0 \quad (3)$$

$$\sum_{j=1}^p b_{kj} = c \quad b_{kj} \geq 0$$

Although this representation is acceptable from an algebraic point of view, it fails to account for the fact that perfect mixing cannot be demonstrated in practice, due to sampling and measurement errors in X . Therefore, it is assumed that the data matrix X is made up of a systematic part X' , attributable to perfect mixing, and a matrix of error terms E , representing non-systematic contributions to X . It is assumed that the errors are relatively small and X' closely resembles X . By definition, the rows of X' , the estimated matrix of perfect mixtures, consist of non-negative linear combinations M of q end-member compositions B :

$$\begin{aligned} X' &= X - E \\ X' &= MB \end{aligned} \quad (4)$$

The range of each variable in X' cannot exceed that of the corresponding variable in the end members B , due to the non-negativity constraint on M . In other words, the end-member matrix contains the extreme values of each variable. By definition, the rows of X' are also subject to the constant-sum constraint, and therefore

$$\begin{aligned} \sum_{j=1}^p x'_{ij} &= c \quad x'_{ij} \geq 0 \\ \sum_{j=1}^p e_{ij} &= 0 \end{aligned} \quad (5)$$

The above considerations lead to the following mathematical formulation of the general mixing model (subject to the constraints listed above):

$$X = MB + E \quad (6)$$

3.3. Inverse modelling strategy

In terms of mathematical modelling, Eq. 6 is the forward model. Once a set of end members is specified, the composition of any mixture can be produced. In case no a-priori information about the number of such end members and/or their compositions is available, the problem is much more complex, and all of the parameters of the mixing process have to be estimated from the data by means of inverse modelling techniques.

The inverse modelling procedure used here consists of two stages. In the first modelling stage, the mixing space is defined by partitioning the data into X' and E ('signal' and 'noise') for each number of end members, following Eq. 4. A matrix of perfect mixtures is generated for every value of q ($2 \leq q \leq p$) using fundamental concepts of linear algebra (singular value decomposition and constrained weighted least squares approximation). Each approximated matrix conforms to the non-negativity constraint of Eq. 5. As will be illustrated in the faunal application below, the 'best' of these solutions is chosen in order to fix X' and q . The dimensionality (shape) of the data in p -space is closely related to the number of linearly independent end-member vectors needed to span the mixing space, indicating that the number of end members can be estimated without knowledge of their compositions. The requirement of linear independence thus limits the maximum number of end members in inverse models of a mixing process to p . In our application the columns of the data matrix were scaled to equal weights prior to the partitioning into signal and noise, so that each variable (i.e. a rodent group) is equally important in determining the approximate dimensionality of the data.

The problem to be solved in the second modelling stage consists of expressing X' , the matrix of perfect mixtures, as the product of two matrices M and B , subject to the constraints of Eq. 3. This is a constrained bilinear minimisation problem, which cannot be solved uniquely without additional infor-

mation. The intrinsic non-uniqueness of the bilinear unmixing solution can be circumvented by specifying additional constraints, based on the trade-off between two apparently contradictory but equally desirable requirements: mathematical and physical (including ecological) feasibility. Of primary concern is that the modeled end members enclose the smallest possible mixing space, so that each end member contributes significantly to the observed compositional variation, and its composition can be easily interpreted in palaeoecological and/or palaeoclimatological terms. However, negative values of end-member contributions are not allowed in the model, and a good fit of the model to the approximated data requires that the number and magnitude of negative contributions are as small as possible. In a geometrical sense, the set of end members must enclose as many of the observations as possible, because any observation not enclosed by the end members is distorted in the modelled representation of the data. The apparent contradiction of these two requirements enables the optimal solution for a given (minimal) value of q to be defined as the smallest possible mixing space which encloses a sufficiently large proportion of the data points.

A new iterative algorithm has been developed for estimating the 'optimal' M and B (Weltje, 1994, 1997). It is more robust, has better convergence properties, and is computationally more efficient than previously developed numerical schemes. Fig. 2 shows the basic concept of the iterative construction of 'optimal' end-member compositions used in this study. The data in the ternary diagram of Fig. 2A consist of three source compositions and six mixtures. The number of end members is thus known a priori. Fig. 2A also shows the locations of three centres of mass in the data set, that have been calculated using a Q -mode cluster algorithm (Full et al., 1982; Bezdek et al., 1984). These centres of gravity are the robust initial end-member estimates employed by the iterative procedure. Because a set of end members has been specified, the matrix of mixing proportions corresponding to these end members can be calculated from the exact bilinear relationship of Eq. 4. This matrix of mixing proportions is evaluated in order to define improvements to the end members, which aim at reducing the number and magnitude of negative mixing proportions. In the next iteration cy-

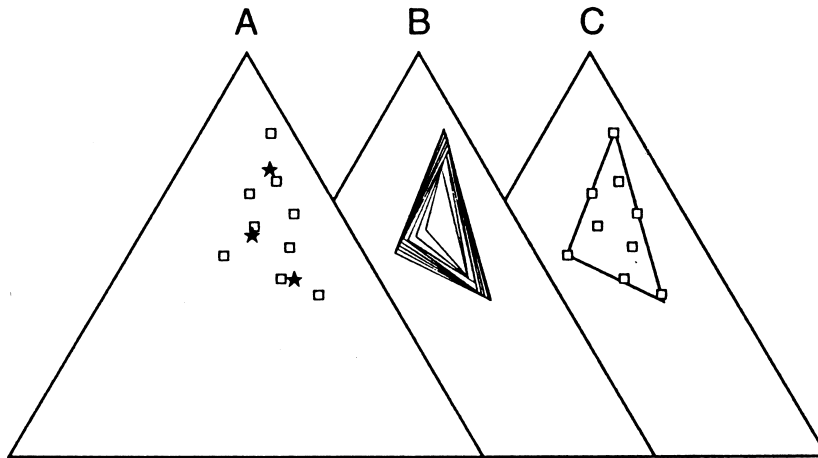


Fig. 2. (A) Synthetic data set consisting of nine three-part compositions. This data set was generated by mixing the three extreme observations in arbitrary proportions in order to generate six additional data points. An initial guess of the end-member compositions (shown as stars) is made by a ‘fuzzy clustering’ algorithm (Full et al., 1982; Bezdek et al., 1984). (B) A series of iteration cycles. The ternary mixing space (represented by a triangle in compositional space) grows in each iteration cycle until the mathematical constraints on a feasible solution have been satisfied. (C) At convergence, the calculated end members are nearly identical to the three extreme observations. The true end members from which the mixtures have been generated are closely approximated. Parameter estimation is independent of sample locations or other considerations, because the mixing model is constructed in compositional space.

cle, the updated matrix of end-member compositions is used to generate a new mixing proportions matrix. In a geometrical sense, the mixing space grows in each iteration cycle, until the constraints on an optimal mixing model have been satisfied (Fig. 2B). Eventually, all of the data points are enclosed by the final mixing space, indicating that the original source compositions are accurately identified (Fig. 2C).

3.4. Palaeoenvironmental extensions to modelling

3.4.1. The nature of the mixing space

It is important to realize that mixing of faunal compositions should not be interpreted as actual physical mixing of teeth. In this respect our application differs from most of the traditional geological and geochemical applications where physical mixing of sediment grains or chemical constituents is described. This application is different because the fossil assemblages are distributed over millions of years and across a broad range of sedimentary systems and basins. The ‘system’ described here is the ecological/climatic system connecting all localities and basins by its control on the geographical and temporal distribution of the rodent groups. Employed in such a way, ‘mixing’ is more conceptual

than physical, and can best be viewed as the result of interaction between climatic factors on the one hand, and adaptations of and interspecific competition between species on the other hand. Although the reality of interspecific competition in communities is still the focus of debate (e.g. see Gotelli and Graves, 1996), its important role in rodents has repeatedly been demonstrated (e.g. Grant, 1972).

3.4.2. Estimation of climatic parameters

The estimation of climatic parameters from rodent end-member compositions is done in three steps: (1) characterizing the end members as ‘cooler’, ‘warmer’, ‘more humid’, etc. on the basis of their compositions; (2) calculating the ratios of the contributions of those pairs of end members which indicate opposite conditions (e.g. ‘cooler’ versus ‘warmer’); and (3) taking the logarithms of these ratios (log-ratios). A log-ratio is the most appropriate form to describe variation within compositions and it is insensitive to closed-sum effects (Aitchison, 1986). A log-ratio of the contributions m_{ik} and m_{il} of the end members k and l (elements of M) to the sample i can be described as:

$$r_{ikl} = \ln(m_{ik}/m_{il}) \quad (7)$$

The log-ratio is undefined when m_{ik} or m_{il} is zero, and in such cases the following decisions are made: if m_{ik} is zero the ratio is set to 0.01; if m_{il} is zero the ratio is set to 100; and in case both m_{ik} and m_{il} are zero the ratio is set to 1.4. The final parameter (e.g. 'relative humidity') is calculated as the first principal component of all selected log-ratios that are used to describe that climatic parameter in step (2).

3.4.3. Palaeoecological assumptions

The following assumptions apply to palaeoecological modelling in general. We subdivide the assumptions into those related to (1) ecological preferences, (2) abundances, and (3) preference–abundance relations. The latter are largely model-dependent.

(1) *Ecological preferences*. It has to be assumed that the ecological and climatic preferences, which are assigned to our a-priori defined palaeoecological rodent groups, and which are primarily based on functional morphological and actualistic principles, are generally valid. Additional uncertainty in ecological preferences of each group is caused by intra-group variation due to evolution and compositional variability within each group. In Section 6.3 we shall demonstrate that the end-member modelling results are insensitive to moderate number of erroneous ecological assumptions.

(2) *Abundances*. The composition of a vertebrate death assemblage is only partly determined by the structure of the original life assemblages, since taphonomic processes may cause serious biases. In this application of end-member modelling the main assumption is that biasing factors operate in a constant way, i.e. that the assemblages are isotaphonomic (Wing et al., 1992). For such a setting, it may be assumed that estimates of relative climate on the basis of the compositions are not disturbed by structural (i.e. constant) under- or overrepresentation of groups. Such a multiplicative perturbation will distort the mixing space spanned by the end-members in an approximately linear way (see Section 6.3). As discussed in van Dam (1997) the assumption of isotaphonomic conditions is reasonable for our data set, the major reasons being that almost all localities are formed in low-energy shallow lacustrine systems, and that the majority of localities comes from a single basin (on which the major part of the final climatic curves is based). In

addition, multivariate outliers will be filtered out during modelling.

(3) *Preference–abundance relations*. The basic assumption is that environments characterized by a large abundance of a certain group are the environments that group actually prefers the most. Similarly, environments where the group is rare or absent are assumed to be environments which are not preferred. Inter-group competition is thought to be the major force behind these relations. The presence of such direct abundance–environment relations implies that communities are in equilibrium with the environment, and that groups react 'instantaneously' to environmental changes. Only then we may expect a one-to-one relation between a specific set of environmental parameters and a certain composition resulting from it. Obviously, the concept of equilibrium is time-scale dependent (Giller and Gee, 1986). However, it is known that even in (geologically instantaneous) ecological time, rodent communities (like most other communities) respond very quickly to environmental changes. This means that in geological time the problem will be even much smaller, because of time-averaging effects within samples.

On the other hand, problems may arise because of the length of geologic time. For instance, tectonic processes may induce the creation or removal of barriers such as mountains and water surfaces. If these barriers prevent groups from reaching certain areas during a part of the studied interval structural zeros will enter the data set. This means in turn that estimates of environmental parameters will be distorted if the absence of these groups would be explained in ecological terms. This problem can be solved by the aggregation of groups, preferably in an ecological way. The result will be that faunal changes caused by the opening of new migration routes will not automatically be expressed in changes in the ecological composition, because the taxa competing or replacing each other may belong to the same ecological category. Structural zeros, representing the not-yet existence or extinction of a group, form another complication. Again, aggregation may solve the problem. Obviously, there is a limit to aggregation, because information is lost every time groups are combined.

More specifically, the underlying model we use to describe the relation between abundances and climatic change between the extreme end-members is

assumed to be of the type described by Eq. 7, which is a monotonously increasing function approximately linear in its central part. (This type of underlying interpolation model should not be confused with the gaussian-type of response models assumed by other methods such as CANOCO and correspondence analysis, which are specified for each individual input group.) The assumption of monotony means for instance that if humidity is known to increase along some geographical gradient, the ratios of ‘humid’ versus ‘arid’ end-member contributions has to increase along this gradient also, i.e. without any reversals. This type of assumptions could be tested by exam-

ining gradients in present-day climate and in rodent compositions and by checking for correlations. Until now we have not performed such a study.

A summary of the methodology is given in Fig. 3. The basic data are relative abundances of first and second molars of rodent species from time-ordered samples from several geological basins (the species relative abundance matrix Y). Species abundances are converted into ecological abundances by grouping species on the basis of diet, locomotion, life history and energy expenditure, and (palaeo)biogeographic distributions (see below). This conversion results in the ecological relative

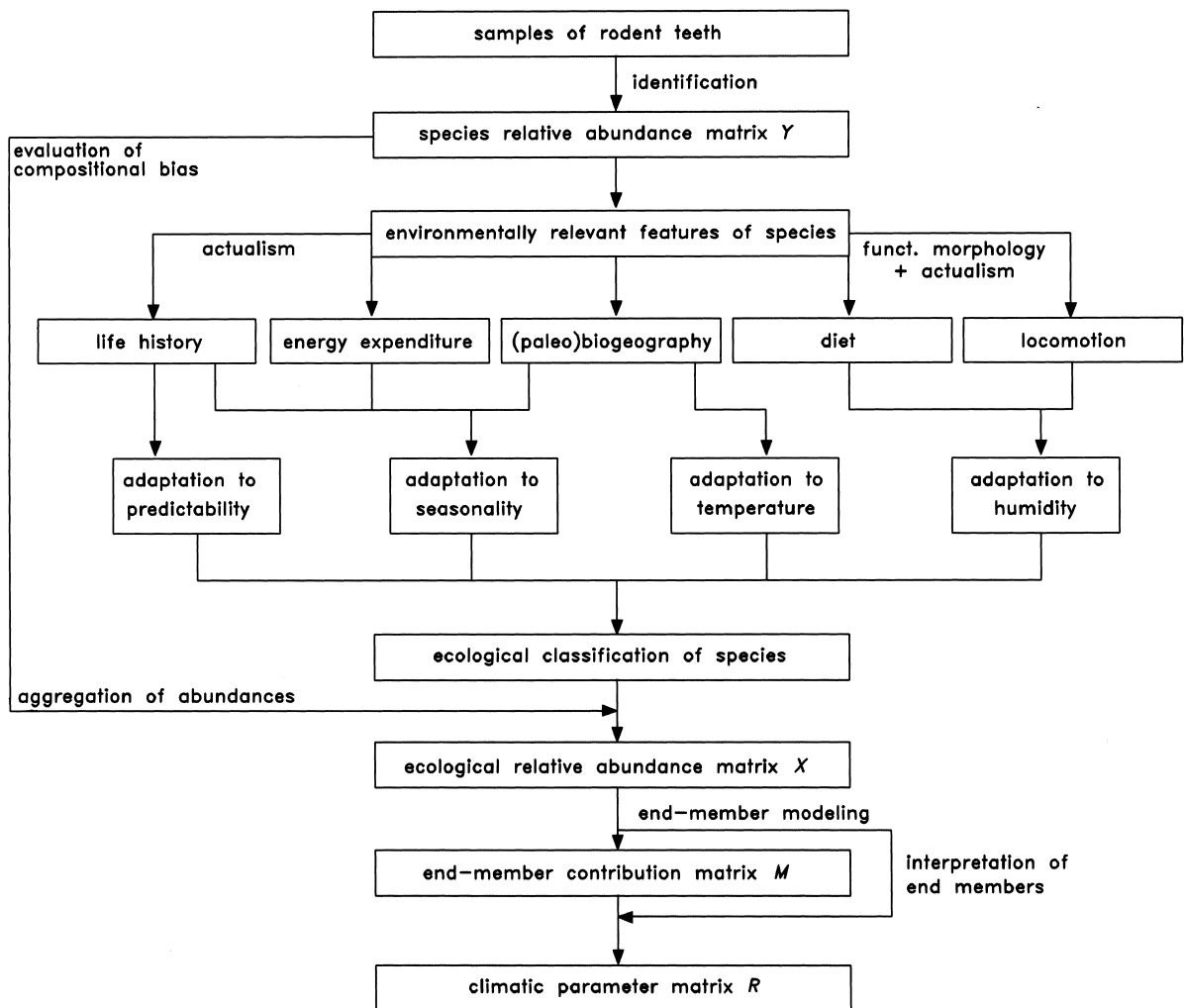


Fig. 3. Methodological flow chart of this study.

abundance matrix X (notation as in Section 3.1). After an evaluation of sources of compositional bias, an end-member model is fitted to X . The matrix M of end-member contributions to the samples is used to calculate climatic parameters (the matrix R).

4. The climatic parameters and their estimation from rodents

Four climatic parameters are estimated on the basis of a fitted end-member model: humidity, temperature, seasonality type and predictability. A general discussion on the use of small mammals as proxies for these parameters is presented in van Dam (1997). Here we restrict ourselves to a short summary, in which we focus on rodents (see also Fig. 3). The inferences of the preferences and adaptations for the particular groups used in the analysis will be discussed in the next section.

Humidity preferences are based on the functional morphology of the dentition, and on the extrapolation of habitats from those of extant relatives (the principle of actualism). Various dental features (hypodonty, brachiodonty, stephanodonty, various types of lophodonty) are interpreted as adaptations to specific diets, which in turn are assumed to indicate certain habitats. Knowledge of extant habitats and phylogenetic relations is used to infer the habitats of fossil relatives.

Temperature preferences are primarily inferred from (a) Miocene palaeobiogeographical distributions, and (b) abundance shifts in Spanish rodents (van der Meulen and Daams, 1992; Krijgsman et al., 1994b) related to the generally accepted global Middle Miocene cooling episode. This cooling followed a late Early to Middle Miocene thermal optimum between 17 and 14.5 Ma (Flower and Kennett, 1993; Hodell and Woodruff, 1994), when Holarctic land temperatures were about 7°C higher than at present (Schwarzbach, 1968; Axelrod and Bailey, 1969; Burchar, 1978; Wolfe, 1994).

Adaptations to inter-annual climatic variability (predictability) are mainly inferred from demographic patterns and associated life-history strategies. (Un)predictability is an important determinant of community structure (Pimm, 1978), and predictable variations in resource availability can be

accommodated by groups with appropriate life histories (Giller and Gee, 1986). We use a demographic tripartition of rodents (French et al., 1975; extensions by van der Meulen and Daams, 1992, and van Dam, 1997) to classify rodents into three groups in terms of adaptations to (un)predictability. The extremely production-oriented species of demographic group 1 (which includes Murinae) are optimally adapted to unpredictable environments. In contrast, strong 'internal clocks' are (or are assumed to be) common in the efficiency-oriented taxa of group 3 (among which are Gliridae, Sciuridae, Petauristidae, Zapodidae and Eomyidae). Such clocks can only function in a predictable environment, because they regulate the tuning of many physiological and behavioural changes to the annual cycle (e.g. hibernation). Representatives of group 2, to which Cricetidae belong, are intermediately adapted with regard to predictability.

Adaptations to seasonality type are based on two considerations. In the first place, the ability to hibernate (Cade, 1964; Precht et al., 1973) is regarded as an adaptation to cool–warm seasonality. The second consideration relates to the climate types and biomes where extant relatives reach their highest diversities. For example murines (group 1) are assumed to have a competitive advantage over many other groups in monsoon-dominated zones, such as savannas, which are areas dominated by wet–dry seasonality. Where monsoon-dominated vegetation zones grade into drier, less productive biomes, murines give way to more survival-oriented groups of group 2, such as gerbils (type 2) in the North African (semi) desert, and cricetines in the Central Asian steppes. Superiority of members of group 3 is typically related to a higher fasting endurance, made possible by large fat stores and hibernation, during which body temperature and activity are lowered. Glirids, which occur in all-year-wet temperate zones dominated by cool–warm seasonality (particularly cold winters), are a good example.

5. Ecological grouping of the rodents

5.1. Ecology and taxonomy

The studied rodent species are classified into nine ecological groups (Table 2). Their relative abun-

Table 2
Ecological grouping of the Late Miocene rodents studied and their assigned scores on climatic parameters

Rodent group			Scores assigned to climatic parameters			
name	ecologically relevant features	taxonomy	humidity (humid: +) (arid: –)	temperature (warm: +) (cool: –)	seasonality (in temp.: +) (in hum.: –)	predictability (high: +) (low: –)
Castoridae	beavers, semi-aquatic	Castoridae	+	–	+	+
Cricetidae I	hamsters with relatively high-crowned molars	Cricetodontini, <i>Blancomys</i>	–	0	0	0
Cricetidae II	hamsters with relatively low-crowned molars	Cricetinae, <i>Megacricetodon</i> ^a	0	0	0	0
Gliridae I	terrestrial dormice with few lophs on molar crowns	Myomiminae except <i>Ramys</i> and <i>Vasseuromys</i>	–	0	+	+
Gliridae II	arboreal/scansorial dormice with many lophs on molar crowns	Bransatoglirinae, Dryomyinae, Glirinae, <i>Ramys</i> , <i>Vasseuromys</i>	+	–	+	+
Muridae I	mice with relatively broad molars with well-developed longitudinal ridges	<i>Occitanomys</i> , <i>Stephanomys</i>	–	0	–	–
Muridae II	mice with relatively slender molars with less well-developed longitudinal ridges	Muridae except <i>Occitanomys</i> and <i>Stephanomys</i> ^b	0	0	–	–
Sciuridae I	ground squirrels preferring relatively open habitats	Xerini	–	+	–	+
Sciuridae II + Eomyidae + Petauristidae	squirrels and eomyids preferring relatively closed habitats	Tamiini, Petauristidae, Eomyidae ^c	+	–	0	+

Positive, neutral and negative scores correspond to high, intermediate/mixed, and low values, respectively (see text for details). Humidity scores are based on diet and locomotion, and temperature scores on Miocene palaeobiogeography. Scores on seasonality type (warm–cool vs. humid–arid) are based on present-day diversities in climatic/vegetational belts and on hibernation abilities. Predictability scores are based on demographic characteristics, reflecting survival- or reproduction-oriented life history strategies.

^a Rest groups *Anomalomys*, *Eumyarion*, *Epimeriones* are included in Cricetidae II.

^b Rest groups Zapodidae and Hystricidae are included in Muridae II.

^c Rest group Marmotini is included in Sciuridae II.

Table 3
Ecological abundance matrix X

Locality	Castoridae	Cricetidae I	Cricetidae II	Gliridae I	Gliridae II	Muridae I	Muridae II	Sciuridae I	Sc. II + Pet. + Eomy.	Total number
KSS	0	5.23	10.47	0	1.16	42.44	40.70	0	0	172
KS	0.65	0	1.06	0	0.24	58.06	39.98	0	0	1228
VDC3	1.02	1.79	4.59	0	0	72.96	19.39	0	0.26	392
MDV7	1.59	0	1.59	0	1.59	92.06	3.17	0	0	63
CC	5.41	8.11	0	0	0	54.05	29.73	0	2.70	37
CC3	0	2.72	0	0	1.97	39.27	51.73	3.09	1.22	1067
LM	0.11	16.91	0.16	0	0.32	72.57	9.18	0.75	0	1863
CC2	0	4.49	0	0	4.49	50.56	38.20	1.12	1.12	89
TO	0	11.36	0	0	0	64.77	17.05	6.82	0	88
VB2	0	0.62	0	0	0	64.71	34.06	0.62	0	323
MDV5	0	2.56	0.51	0	1.03	46.41	43.59	1.54	4.36	390
MDV4	0	5.13	0	0	0	51.28	41.03	0	2.56	39
TOD	0	7.08	0	0	0	49.56	40.71	0	2.65	113
TOC	0	4.17	0	0	4.17	12.50	79.17	0	0	24
MDV3	0	3.33	0	0	0	26.67	70.00	0	0	30
CCB	0	2.08	0	0	4.17	54.17	39.58	0	0	48
MDV2	0.43	5.25	1.29	0	0.75	44.59	45.55	0.64	1.50	933
LM2	0	31.58	2.63	0	0	55.26	10.53	0	0	38
VIP	0	7.40	0.24	0	0	80.43	11.93	0	0	419
TOA	0	9.31	1.06	0	0.53	76.06	13.03	0	0	376
AG3	0	6.01	1.09	0	0.55	68.85	23.50	0	0	183
ALF	0	0	1.85	0	0	72.22	25.93	0	0	54
PM3	0	19.12	1.47	0	0	58.82	20.59	0	0	68
GLO10	0	6.62	1.32	0	0.66	70.20	21.19	0	0	151
AG1	0	4.07	0	0	0	89.43	6.50	0	0	123
PERD	0	17.04	0	1.48	0	0	81.48	0	0	135
PERC	0	15.45	0	0	0.28	0	84.27	0	0	356
R2	0	7.14	2.38	2.38	0	0	88.10	0	0	42
PM2	0	29.27	2.44	2.44	2.44	0	60.98	2.44	0	41
ROM11	0	4.93	1.41	0.70	1.41	0	91.55	0	0	142
MBB	0.47	23.94	0.23	1.41	1.64	0	72.07	0.23	0	426
PER4	0	6.38	0	12.77	2.13	0	78.72	0	0	47
ROM9	0	5.08	0	6.78	5.08	0	83.05	0	0	59
MBA	0	19.57	0.72	3.62	4.35	0	71.74	0	0	138
ROM7	0	18.75	2.50	16.25	1.25	0	61.25	0	0	80
ROM4C	0	7.14	0	22.86	0	0	70.00	0	0	70
ROM3	0	28.07	19.30	47.36	0	0	0	0	5.26	57
PER5	0	51.81	10.84	37.53	0	0	0	0	0	83
CU	0	15.55	0	0	0	57.42	27.03	0	0	418
CASAL	0.71	42.76	35.69	18.37	0.35	0	0	1.77	0.35	283
PED2C	0	22.17	62.43	4.84	9.36	0	0.11	0.65	0.43	929
PED2A	3.09	46.34	25.04	13.33	10.41	0	0	1.79	0	615
CAR1	1.86	18.58	63.62	12.53	3.41	0	0	0	0	646
NOM	0.81	37.25	44.94	13.77	0.40	0	0	2.83	0	247
CR5	0	9.00	13.00	0	2.00	30.00	32.00	0	14.00	100
CR4	0	1.16	31.40	0	0	17.44	50.00	0	0	86
CR3	0	2.00	19.00	0	2.00	44.00	31.00	2.00	0	100
CR2	0	1.46	28.64	0	0.97	24.76	40.78	3.40	0	206
CR1	0	0	23.38	0	2.60	37.66	35.06	1.30	0	77
TNA	0	1.54	75.38	0	1.54	0	1.54	0	20	65
TSA2	0	13.64	56.82	0	0	0	15.91	0	13.64	44

Table 3 (continued)

Locality	Castoridae	Cricetidae I	Cricetidae II	Gliridae I	Gliridae II	Muridae I	Muridae II	Sciuridae I	Sc. II + Pet. + Eomy.	Total number
CL	0.76	6.44	85.98	0	1.33	0	0.38	1.89	3.22	528
CP	1.67	64.02	15.06	0.84	2.09	0	0	13.81	2.51	239
HSS	0	52.15	21.47	2.45	0	0	0	23.93	0	163
TOR1	7.27	5.45	0	0	20.00	0	67.27	0	0	55
MONTR	0	3.04	63.69	0	9.22	0	22.03	1.47	0.55	1052 ^b
CUCS	0	4.20	4.90	0	1.40	72.03	16.08	0	1.40	143 ^a
LS	0	0	1	0	29	1	68	0	1	3099 ^a
DION	2	11	5	0	4	0	71.5	0.25	6	1249 ^a
AMB3	0	0	34	0	10	2	29	0	25	126 ^a
AMB2	0	2	41	0	7	0	38	0	12	567 ^a
AMB1	0.25	9	22	0	8	0	53.75	0	7	341 ^a
SOBL	2	0.16	32.84	0	6	0	39	0.25	19.75	612 ^a
DOUVR	2	0	40	0	5	0	32	0	21	95 ^a
EICHK	0.08	0	34.5	3.17	8.87	0	45.57	0	7.81	1230 ^a
PK4	0	9.28	3.09	14.44	1.03	15.46	56.7	0	0	97
LEF	0	13.64	4.55	3.03	4.55	0	71.21	0	3.03	66

Totals are numbers of first and second molars, unless indicated otherwise. Prior to modelling, zeros are replaced by small values corresponding to half a tooth (which is the measurement error).

^a Totals are numbers of first, second and third molars; proportions are based on these numbers.

^b Proportions are based on first and second molars for Gliridae and on first molars for other groups.

dances (the matrix X in Fig. 3) are shown in Table 3 and Fig. 4. Families are considered to represent certain 'ways of life', which are related to their demography and energy expenditure strategies as discussed above. Most families are split into two groups according to preferences for open or closed habitats, based on inferred diet (Cricetidae, Gliridae, Muridae) or locomotion (Gliridae, Sciuridae). As a result, ecological and taxonomic boundaries coincide in the Sciuridae, whereas in Gliridae the ecological boundary runs through a subfamily (see the description of the nine groups below). Because of the uncertain taxonomic status of *Blancomys* in the Cricetidae it is difficult to ascertain whether the ecological boundary in this family corresponds to a taxonomic boundary. No tribes or subfamilies have been defined for the Muridae studied here.

Overall, phylogenetic relations within each of the nine groups are tight. This has the additional advantage that most of them also function as geographical units, facilitating the attribution of temperature preferences. The close relation between taxonomy and ecology in our data set is in agreement with the general notion that ecological designations tend to include closely related species (Simberloff and Dayan,

1991). Our final grouping may be regarded as the result of a consensus between ecological, taxonomical, and statistical considerations (with the latter resulting in aggregation of genera, as discussed in the previous section). An important asset of this subdivision is that each group is characterized by a unique set of preferences in Table 2, implying that each group occupies a unique position in 'ecological space'.

5.2. Scores on preferences and adaptations

Adaptations or preferences are assigned in the form of positive (+), neutral (0) or negative (–) scores (Table 2), and follow the principles mentioned in Section 4. For clarity, a remark has to be made on the temperature scores. A neutral score in Table 2 indicates a Late Miocene geographical distribution which was restricted to, or had its centre at the latitude of Spain, i.e. the northwestern part of the Mediterranean area. A positive score is assigned to groups whose Late Miocene distribution had a major extension into lower latitudes (Africa), and/or showed a decline in Spain during the Middle Miocene cooling. Similarly, a negative score is assigned to groups that had their centres of distri-

Ecological groups (Rodentia)

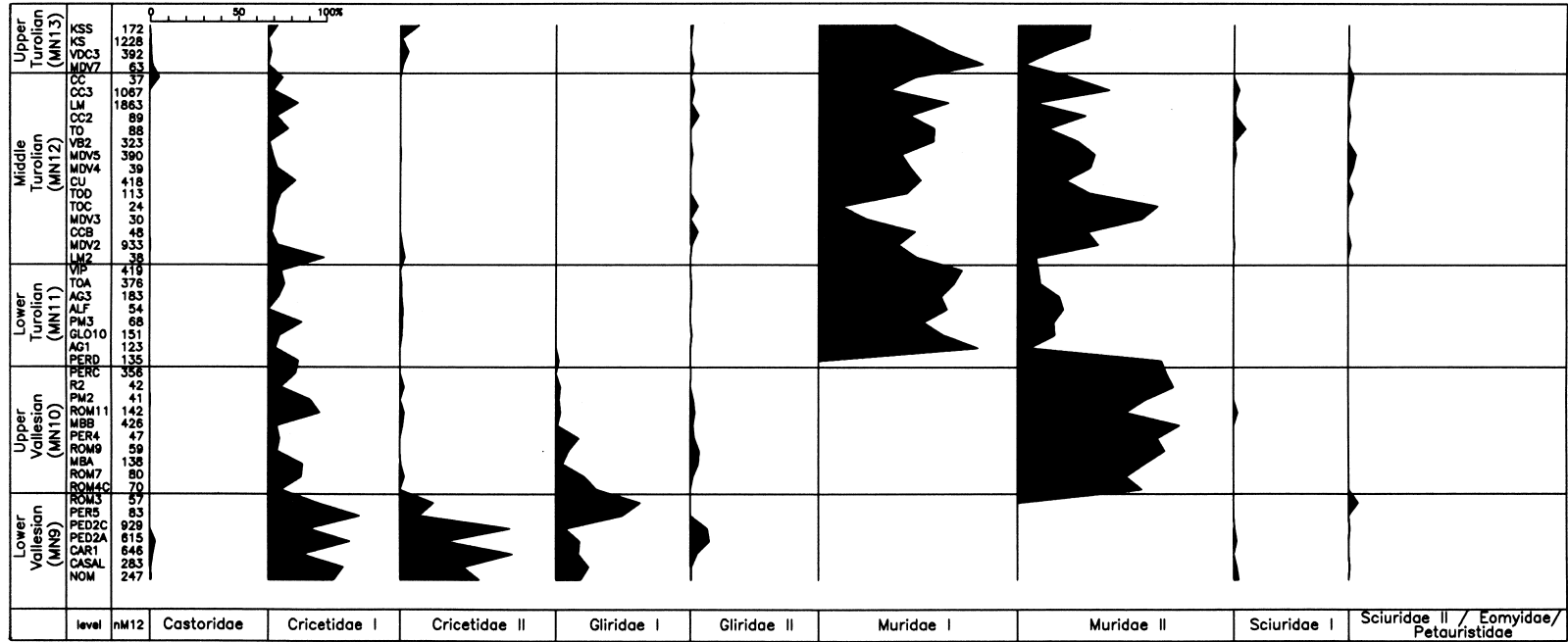


Fig. 4. Relative frequencies of ecological groups in the Calatayud–Daroca and Teruel basins (together representing a large part of the ecological relative abundance matrix X).

bution at higher (central European) latitudes, and/or increased their numbers and/or diversity during the Middle Miocene cooling. Unfortunately there is no Miocene rodent record for high-latitude areas, but indirect evidence for at least the temporary presence of a group at high latitudes is indicated by occurrences in both Eurasia and North America, implying intercontinental migration across the Bering Street.

We admit that some +, 0 and – assignments are tentative or may even be wrong. However, we will show that the method is robust against a limited number of errors in the assignments (Section 7.3).

5.3. The nine groups (Tables 2 and 3 and Fig. 4)

The nine rodent groups and their preferences and adaptations will now be described.

(1) **Castoridae**. In spite of their rareness in the associations studied here, beavers are kept as a separate group because of their specific ecological requirement for permanent open water. Beavers are given a negative score for temperature, because their Late Miocene palaeobiogeographic distribution includes the mid-latitudes, and because their fossil record indicates repeated migration across the Bering Street (Korth, 1994). Their score on seasonality type is positive because the present-day distribution of beavers can be associated with the middle- to high-latitude zones of cool–warm seasonality. Their score on predictability is positive because of their high life expectancies.

(2) Relatively high-crowned Cricetidae (**Cricetidae I**) (use of Cricetidae according to Chaline et al., 1977). Late Miocene Cricetodontini (*Hispanomys*, *Ruscinomys*, *Byzantinia*) and *Blancomys* are included because of their hypsodonty and similar geographic distribution. Their hypsodonty is interpreted as an adaptation to diets containing a significant proportion of fibrous plant parts, including grasses. Because of this, a preference for open, more arid environments is assumed (de Bruijn et al., 1993). A neutral score on temperature is assigned because the records from Spain (MN9–13), Greece and Anatolia (MN9–12) show that the southern part of western Eurasia was the main area where the mentioned genera lived then (de Bruijn et al., 1993). Seasonality and predictability preferences are assumed to be identical to those of the Cricetidae II group (see

below). There is one occurrence of *Cricetodon* in the dataset (*C. lavocati* from HSS). Although the species is less hypsodont than the other members of the group, we included it into Cricetidae I because of its resemblance to other Cricetodontini in terms of the robustness and general habitus of the molars.

(3) Relatively low-crowned Cricetidae (**Cricetidae II**). This heterogeneous group includes all Cricetidae in the data set which do not belong to Cricetidae I. The most abundant genera are *Megacricetodon*, *Cricetulodon*, *Rotundomys* and *Kowalskia*. The group is not split up in order to prevent a high frequency of structural and statistical zeros in the data matrix. A neutral score is assigned to humidity, because some genera are assumed to prefer more open, others to prefer more closed habitats, while still others do not seem to have any preference (Daams et al., 1988). An intermediate temperature preference is assigned. Some genera were more restricted to southern Europe (*Cricetulodon*–*Rotundomys*), whereas others had distribution areas across both south and central Europe (*Megacricetodon*, *Kowalskia*, *Cricetus*).

A neutral score on seasonality type is assigned to this group on the basis of the diversity patterns of the two extant groups of Cricetinae and Peromyscini. Cricetinae are particularly successful in the Asiatic steppes. Generally, these areas have a wet–dry seasonality which is less extreme than in savannas. Cool–warm seasonality is rather strong also, and weak hibernation occurs in a number of genera (*Cricetus*, *Mesocricetus*). Cool–warm seasonality is not so strong in the Mexican steppes, where peak diversities of extant Peromyscini occur (Nowak, 1991). Neither is hibernation known for this tribe. Nevertheless, we will test also for a positive score on seasonality type, i.e. for an adaptation to cool–warm seasonality. Because of their membership to the intermediate demographic group 2, a neutral score on predictability is assigned.

(4) Ground-dwelling Gliridae (**Gliridae I**) (use of Gliridae after Daams and de Bruijn, 1995). This group consists of dormice with molars that have occlusal surfaces with a relatively low number of transverse crests. This dental feature is observed in the extant ground-dwelling dormouse *Myomimus* and many extinct representatives of the subfamily Myomiminae, and is thought to be indicative of a life

on the ground and of an open, relatively dry habitat (van der Meulen and de Bruijn, 1982; Daams and van der Meulen, 1984). The Gliridae I group consists of the three Myomiminae genera *Myomimus*, *Miodyromys* and *Tempestia*. Two other Myomiminae have many ridges (*Vasseuromys* and *Ramys*). We follow the interpretation of Daams and van der Meulen (1984) and include these into Gliridae II.

An intermediate score is assigned to temperature. Although the Myomiminae were flourishing across Europe during the Early and Middle Miocene, Late Miocene genera had a more restricted distribution. *Myomimus* is documented from Spain to Pakistan, but its absence in the Late Miocene localities of France of our data set shows that it had a limited north–south range in Europe during this period. Similarly, *Miodyromys* was widespread across Europe during the Early–Middle Miocene in Europe, but its later Miocene occurrence was restricted to southern areas (Vallès-Penedès, Spain, early MN9). *Tempestia* was endemic to Spain. On the basis of the occurrence of hibernation in *Myomimus* a preference for cool–warm seasonality is assigned. Because of their membership to demographic group 3, a positive score on predictability is assigned.

(5) Arboreal/scansorial Gliridae (**Gliridae II**). This group includes representatives of the subfamilies Glirinae (*Glis*, *Muscardinus*, *Myoglis*, *Glirudinus*), Dryomyinae (*Eliomys*, *Glirulus*, *Microdyromys*, *Paraglrulus*) and Bransatoglirinae (*Bransatoglis*), as well as the two Myomiminae genera mentioned above (*Vasseuromys*, *Ramys*). A positive score on humidity is attributed to Gliridae II because of their assumed arboreal (canopy-dwelling) or scansorial (sub-canopy climbing) way of life, which is attributed to the group on the basis of the habitats of extant relatives, and a molar morphology characterized by many transverse crests (Storch, 1978; van der Meulen and de Bruijn, 1982; Daams and van der Meulen, 1984). The rare dryomyine *Graphiurops* is not separated from the other genera of its subfamily, although its molar pattern with relatively few ridges suggests that inclusion in Gliridae I would perhaps have been better. A negative score on temperature is assigned because relative abundances and diversity of forms with many-lobed molars are small in the Late Miocene in Spain compared with contemporary associations from more northern areas

(Mayr, 1979; Mein, 1984). A preference for cool–warm seasonality is ascribed to this group because maximum diversities occur in the temperate zones of Eurasia and because they show the habit of deep hibernation. The predictability score is positive as in the previous group.

(6) Muridae of the *Occitanomys*–*Stephanomys* group (**Muridae I**). (Use of Muridae according to Chaline et al., 1977.) Stephanodonty (Schaub, 1938) is well developed in this group. The stephanodont pattern is characterized by a garland-type pattern of ridges between the posterior cusps of the upper molars. The well-developed longitudinal valleys indicating a strong power stroke (van Dam, 1996) and the relatively large width–length ratios of the molars (van Dam, 1997) indicate a diet which at least partly consists of fibrous components. It is therefore suggested that the group is adapted to relatively open and dry environments. An intermediate temperature preference is assigned to both genera because their Late Miocene distribution was almost exclusively restricted to southwestern Europe (*Stephanomys*) and southern Europe and Anatolia (*Occitanomys*) (de Bruijn et al., 1996). Seasonality and predictability scores are identical to those of Muridae II (see below).

The Muridae I group is the only group with structural zeros in the data matrix, because it was non-existent during the Vallesian (MN9–10). However, its unique combination of adaptations and preferences (Table 2) is not shared with any of the other groups living in the Vallesian, so it may be argued that the group was adapted to a type of environment that was not yet existing by then.

(7) Muridae: *Progonomys*, *Huerzelerimys*, *Parapodemus* and *Apodemus* and some rare *Castromys* and *Rhagapodemus* (**Muridae II**). Although *Rhagapodemus* becomes more and more high-crowned during its evolution, we include it into this group because the representatives in our data set are primitive, relatively low-crowned and resemble *Apodemus* very much.

A neutral humidity score is given to this group. The only still living genus, *Apodemus*, is tolerant to different kinds of habitats. Most of its species have broad frugivorous to omnivorous diets, but do not graze (Niethammer and Krapp, 1978; Nowak, 1991). A biometric analysis on cheek teeth of extant and fossil murids (van Dam, 1997) suggests that

Progonomys, *Huerzelerimys*, and *Parapodemus* were not grazing rodents either.

An intermediate temperature preference is assigned to Muridae II because of their relatively high abundances and diversity in southern Europe during the Late Miocene. This means that we do not regard the recent high diversity of murids in tropical areas as an indication of a high-temperature preference of Miocene Murinae. A negative score on seasonality type is assigned to Muridae because they reach their highest present-day diversities in vegetation zones characterized by a wet–dry monsoon-seasonality, such as savannas. Unfortunately for our purposes, Montuire (1994) did not include annual differences in precipitation as a parameter in her study on the relation between extant murid diversity and climate. However, these authors did find a negative correlation between murid diversity and the annual difference in temperature. This is consistent with our negative score on cool–warm seasonality.

We consider the rare Zapodidae of age MN11 as a rest group and combine them with the Muridae, which is the most abundant family in Spain at this time. Assignment to Muridae II group is preferred, because the presence of Zapodidae is more correlated to the presence of *Parapodemus* (Muridae II) than to *Occitanomys* (Muridae I) in the data set. Hystricidae occur only in one locality (Las Casiones, Teruel basin) and are also included into this group.

(8) Sciuridae: ground squirrels of the tribe Xerini (**Sciuridae I**). The ground squirrels *Heteroxerus* and *Atlantoxerus* are assumed to be indicators of relatively open habitats and hence low humidity. The two extant *Xerus* species are living in the drier savannas, and the NW African relict species *Atlantoxerus getulus* lives in an arid mountainous environment (Kingdon, 1974; Nowak, 1991). A positive score on temperature is assumed for Xerini, because they flourished during the late Early to Middle Miocene thermal optimum in Spain and declined during the subsequent Middle Miocene cooling episode (Daams et al., 1988). A positive score on temperature is supported by the regular occurrence of *Atlantoxerus* in the Upper Miocene of the Maghreb (Jaeger, 1977; Coiffait, 1991).

Adaptation to wet–dry seasonality is assumed because of the adaptation of extant *Xerus* to savanna environments (Kingdon, 1974). Xerini are not known

to hibernate, and it is uncertain whether they possess any type of torpidity (Cade, 1964). Being Sciuridae, their energy expenditure strategy may be expected to be relatively survival-oriented. The positive score of Xerini on predictability is assigned because of their assumed membership to demographic group 3.

(9) Sciuridae: ground squirrels of the tribe Tamiini (**Sciuridae II**), flying squirrels of the family **Petauristidae**, and **Eomyidae**. All three taxa are put in one group because of their supposed common preference for forested environments, and the low abundances of each individual subgroup. It is assumed that the extinct genus *Spermophilinus*, like the majority of extant Tamiini (Nowak, 1991), preferred closed, relatively humid biotopes. This assumption is consistent with the high abundances of *Spermophilinus* in very ‘wet’ faunas such as Dorn–Dürkheim in the German Rhine basin (Franzen and Storch, 1975). Undoubtedly, flying squirrels were adapted to a life in forests like their extant relatives. Eomyids are extinct, but there are sufficient indications that they preferred closed vegetation (Daams et al., 1988; van der Meulen and Daams, 1992 and unpublished data). The recent discovery of a flying membrane on a Late Oligocene eomyid (Storch et al., 1996) from Germany is in agreement with this hypothesis. The shared biotope preference of *Spermophilinus*, Petauristinae and Eomyidae is confirmed by their simultaneous occurrences in (the more northern localities in) our data set.

This ninth group is given a negative score for temperature. *Spermophilinus* is a very common element in Late Miocene northern localities such as Dorn–Dürkheim in the Rhine basin and Eichkogel in the Vienna basin. During the late Early to Middle Miocene thermal optimum the genus is temporarily absent in Spain (van der Meulen and Daams, 1992; unpublished data), whereas it is present at higher latitudes (e.g. Puttenham). Today, Tamiini are particularly successful in North America. An adaptation to cool environments is indicated by their apparent migration across the Bering Street. The Eomyidae are a similar case. This family was especially abundant in Spain during the Late Oligocene–Early Miocene (Alvarez Sierra, 1987). The detailed record from the CT basins shows that they disappeared during the thermal optimum, but reappeared afterwards in MN6 (Manchones, Las Planas 5K, see Daams et al., 1988)

and MN 9 (Masía de la Roma 3, see van Dam, 1997). In more northern areas, however, Eomyidae bridge the interval in which they were absent in Spain (Engesser, 1990; Bolliger, 1992; Fahlbusch and Bolliger, 1996). The group remains well-represented at relatively high latitudes during younger intervals. For example, three different genera occur in Podlesice in Poland (Fahlbusch, 1978). A northern transcontinental migration route is assumed for the Eomyidae, because of their supposed North American origin (Fahlbusch, 1979; Korth, 1994). Petauristidae are today particularly diverse in tropical South-East Asia, but during the Neogene they flourished in forested areas all across central Europe (de Bruijn, 1995), and showed a high diversity in latitudes at least as high as Poland (Kowalski, 1990).

A tentative neutral score is given to seasonality type. Whereas present-day diversity of Tamiini is

high in (cool–warm seasonal) temperate zone forests (e.g. western United States), hibernation is weak and accompanied by food hoarding. Petauristinae are particularly diverse in tropical SE Asia and do not hibernate. Information is absent for the extinct Eomyidae. The predictability score of the complete group is positive because all subgroups belong to demographic group 3.

6. Model results

6.1. End-member interpretation

Fig. 5 shows goodness of fit statistics (R^2 values) for each rodent group as a function of the number of end members. A mixing model with four end members seems to be a reasonable choice consid-

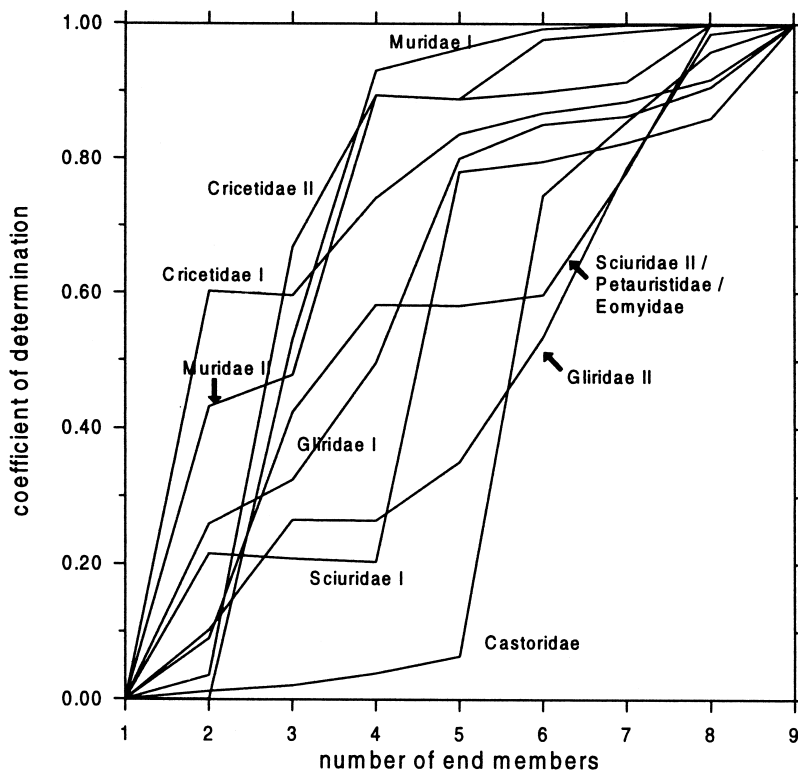


Fig. 5. Goodness of fit for ecological groups as a function of the number of end members. Estimating the number of end members is the first step in the modelling procedure. The number of end members is equal to the smallest number of dimensions required for a reasonable approximation of the data set. This approach does not require any knowledge of the end-member compositions. The curves show that some of the variables can be reproduced fairly well with only two end members. A four end-member model is a reasonable minimum scenario.

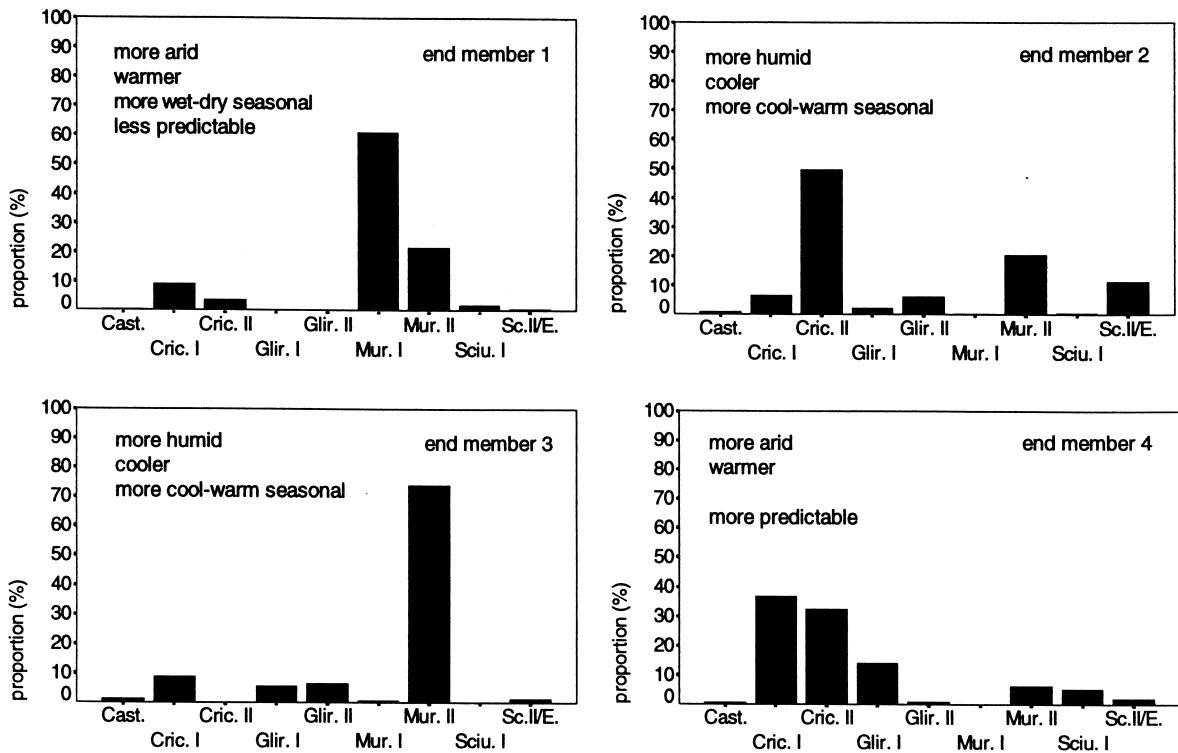


Fig. 6. The four end-member compositions and their climatic interpretations. For further explanation see text. Note that the group indicated as *Sc.II/E.* (Sciuridae II–Eomyidae) also includes the Petauristidae.

ering the level of noise on the one hand, and the desire for a simple description on the other hand. This model implies a very low goodness of fit for the Castoridae, which means that variation in this group is mainly regarded as noise. The remaining groups are adequately reproduced, although Sciuridae I and Gliridae II show a lower goodness-of-fit than other groups.

The four end-member compositions are shown in Fig. 6 and Table 4. In addition, Table 4 shows how the end members are interpreted in terms of climate. If a group has a positive score on a specific parameter in Table 2, it scores positively (+) on the end members containing a large proportion of this group compared to other end members (row-wise comparison in Table 4). Similarly, a positive score in Table 2 results in a negative (–) or neutral (0) score in Table 4 in case of low or intermediate proportions, respectively. The same reasoning applies to negative scores in Table 2. Neutral scores in Table 2 always translate into neutral scores in Table 4.

The net scores for the end members enable a straightforward interpretation, because in most cases the scores of the nine ecological groups appear to point in the same direction, allowing the identification of ‘humid’, ‘warm’, etc. end members. Here we regard net scores higher than 1 or lower than –1 as indicative, which implies that we attribute four climatic characteristics to end members 1 and 4, and three to 2 and 3. It appears that end members 1 and 4 can be described as relatively dry and warm, whereas 2 and 3 can be described as relatively humid and cool. End members 2 and 3 are at the same time characterized by cool–warm seasonality, whereas 1 is characterized by wet–dry seasonality. End member 1 can also be described as unpredictable, and 4 as predictable.

Table 5 shows the end-member contributions for all localities, while Fig. 7 shows the contributions for the subset of localities from the CT basins. *End member 1* is an (extreme) Spanish ‘Turolian’ composition, containing more than 80% murids and no

Table 4
End-member compositions and climatic interpretations

Group	End member																			
	1					2					3					4				
	%	H	T	S	P	%	H	T	S	P	%	H	T	S	P	%	H	T	S	P
Castoridae	0.67	–	+	–	–	1.07	0	0	0	0	1.51	+	–	+	+	0.77	–	+	–	–
Cricetidae I	9.44	+	0	0	0	6.77	+	0	0	0	9.10	+	0	0	0	36.92	–	0	0	0
Cricetidae II	3.76	0	0	0	0	49.99	0	0	0	0	0.00	0	0	0	0	32.62	0	0	0	0
Gliridae I	0.00	+	0	–	–	2.43	+	0	–	–	5.91	0	0	0	0	14.41	–	0	+	+
Gliridae II	0.00	–	+	–	–	6.37	+	–	+	+	6.93	+	–	+	+	1.21	–	+	–	–
Muridae I	61.22	–	0	–	–	0.44	+	0	+	+	0.75	+	0	+	+	0.00	+	0	+	+
Muridae II	21.77	0	0	+	+	20.54	0	0	+	+	74.18	0	0	–	–	6.54	0	0	+	+
Sciuridae I	2.20	0	0	0	0	0.69	+	–	+	–	0.00	+	–	+	–	5.38	–	+	–	+
Sciuridae II + Petauristidae + Eomyidae	0.94	–	+	0	0	11.70	+	–	0	0	1.61	–	+	0	–	2.15	–	+	0	0
Net score		–	+	–	–		+	–	+	+		+	–	+			–	+		+
		2	3	3	3		6	3	3	1		4	2	3	0		5	4	0	2
Relative climate	arid					humid					humid					arid				
	warm					cool					cool					warm				
	wet–dry seasonal					cool–warm seasonal					cool–warm seasonal									
	predictable															predictable				

Interpretations are based on the total net score of +, – and 0 scores calculated across columns. The individual scores are determined as follows. A positive score of a group in Table 2 may translate into a positive, negative or neutral score on an end member in this table, if the group has a high, low or intermediately high proportion, respectively, in the end member, relative to other end members (comparison along rows of this table). Similarly a negative score in Table 2 may translate into a negative, positive or neutral score. A neutral score in Table 2 will always translate into a neutral score in this table. H = humidity; T = temperature; S = seasonality type; P = predictability.

glirids. Its composition resembles mostly that of the lower Turolian localities of the CT basins, to which it contributes more than 90%. *End member 2* is identical to the (filtered) compositions of AMB3 (Rhône basin, lower Turolian) and TNA (Vallès-Penedès basin, upper Vallesian). It is a relatively northern, humid end member containing significant numbers of both cricetids and murids (Fig. 6). With a proportion of 50%, cricetids are the dominant family. The low humidity-adapted Cricetidae I and Muridae I groups are scarce. Humid groups such as the Gliridae I and Sciuridae II–Petauristidae–Eomyidae group score high. *End member 3* closely resembles the late Vallesian compositions from the CT basins (ROM9, ROM11), Duero basin (TOR1) and Greece (LEF), but some of the younger middle Turolian localities such as TOC (CT basins) and PK4 (Greece) show a high contribution of end member 3 as well. Approximately 75% of the composition of this end member consists of the Muridae II group, whereas the Cricetidae II group is totally absent (Fig. 6). Both

glirid groups are well-represented, whereas Xerini (Sciuridae I) are absent. Finally, *end member 4* has a composition which is typical for early MN9 localities (NOM and CASAL from the CT basins, and HSS and CP from the Vallès-Penedès basin), and several latest MN9 localities (PER5 and ROM3 from the CT basins). Cricetidae are dominant in this fourth end member (~70%), with about equal representations of high- and low-crowned groups. Very characteristic are the peak abundances for the ground-dwelling groups Gliridae I and Sciuridae I, and the very low numbers of Muridae.

Fig. 8 compares input and estimated model output for the CT basins. This figure shows that a significant amount of noise has been removed from the data. The general smoothing effect is shown by the reduction of extreme values. In some individual cases, filtering leads to pronounced modifications in proportions: for instance, a 45% maximum in terrestrial Gliridae (Gliridae 1) is not recognized as relevant in the model, and completely eliminated. An interesting

End-member contributions

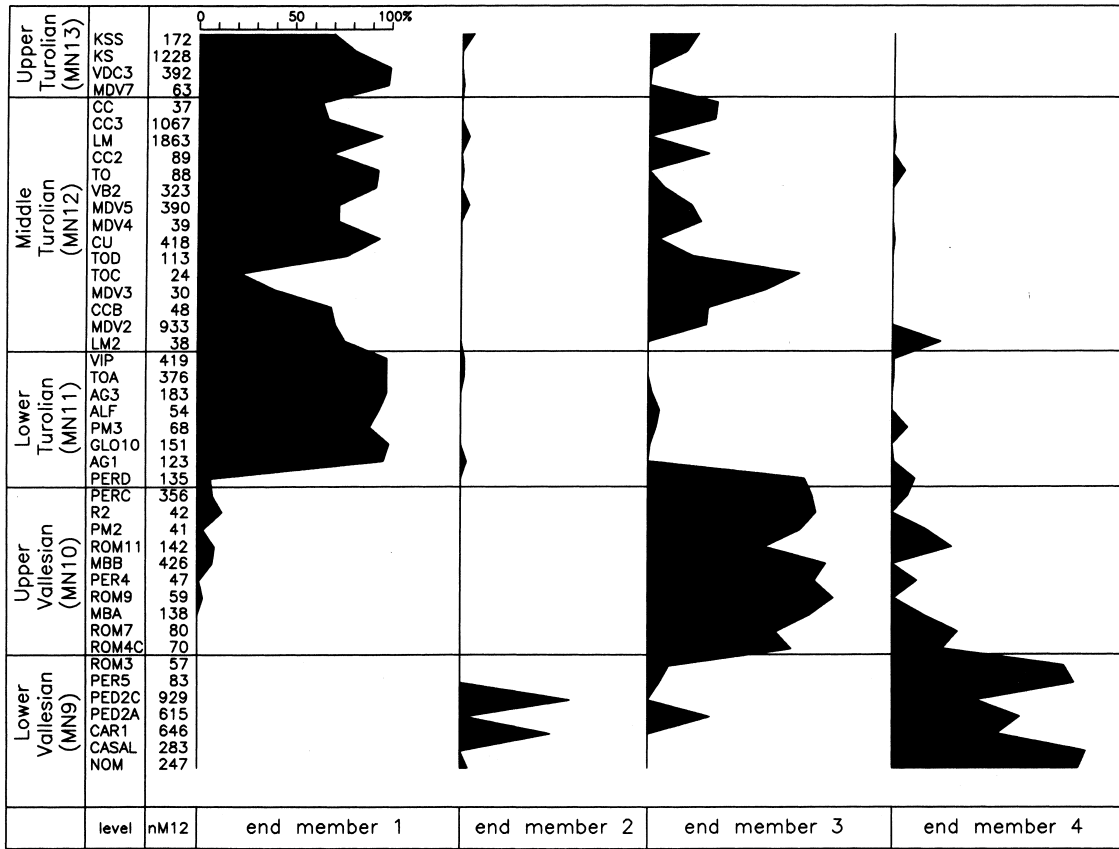


Fig. 7. End-member contributions to the compositions of the localities from the Calatayud–Daroca and Teruel basins (together representing a large part of the end-member contribution matrix *M*).

result is the consistent generation of proportions up to 7% of Muridae I (*Occitanomys/Stephanomys*) just before their actual entry in the early Turolian. Supposedly, on the basis of the covariations between all groups, the model ‘expects’ already some Muridae I in the late Vallesian (note that time is not included in the model, but only added afterwards). This presence is acceptable, given the gradual morphological change from *Progonomys hispanicus* (Muridae II) leading to *Occitanomys* (Muridae I) during this interval (van de Weerd, 1976; van Dam, 1997). A similar effect occurs in Muridae II, which show substantial estimated proportions (in one case even 28%) during MN9, although it is still an extremely rare group by then. The interpretation could be that the environment was suitable for this group in prin-

ciple, but that some other factor may have prevented the group from becoming abundant (which implies the violation of model assumptions 1 and 2, see Section 3.4.3). Fig. 8 also shows that proportional variation in the rare Castoridae and the Sciuridae II/Eomyidae group are largely interpreted as noise for the CT basins. Particularly the latter group is more abundant in other basins, where its abundances are not interpreted as noise.

6.2. Climatic parameter estimation

As explained above, the final values of the climatic parameters (Table 5) are based on log-ratios of end members with opposite interpretations. For each parameter, those end-member pairs are selected

Table 5
Estimated end-member contributions and climatic parameters

Locality	Contribution of end member (total = 1)				Climatic parameter (relative values)	
	1	2	3	4	humidity = –temperature	predictability = cool/warm seasonality = –wet/dry seasonality
<i>Teruel–Alfambra region, Teruel basin, Spain</i>						
KSS	0.696	0.056	0.248	0	0.12	–0.65
KS	0.806	0	0.194	0	–0.46	–0.95
VDC3	0.990	0	0.010	0	–1.27	–1.42
MDV7	0.983	0.013	0.004	0	–1.20	–1.39
CC	0.643	0.003	0.353	0	–0.24	–0.79
CC3	0.665	0	0.335	0	–0.26	–0.81
LM	0.949	0.040	0	0.011	–0.90	–1.22
CC2	0.694	0	0.306	0	–0.30	–0.84
TO	0.929	0.009	0	0.062	–1.72	–1.19
VB2	0.919	0	0.081	0	–0.72	–1.12
MDV5	0.732	0.044	0.224	0	0.02	–0.72
MDV4	0.725	0.003	0.272	0	–0.34	–0.87
TOD	0.770	0	0.230	0	–0.40	–0.91
TOC	0.223	0	0.777	0	0.27	–0.28
MDV3	0.404	0	0.596	0	0.03	–0.54
CCB	0.690	0	0.310	0	–0.29	–0.83
MDV2	0.705	0	0.295	0	–0.31	–0.85
LM2	0.755	0	0	0.245	–1.96	–0.92
VIP	0.975	0.020	0	0.005	–0.91	–1.42
TOA	0.978	0.018	0	0.004	–0.94	–1.43
AG3	0.984	0	0.016	0	–1.15	–1.36
ALF	0.941	0	0.059	0	–0.81	–1.17
PM3	0.885	0	0.037	0.078	–1.40	–0.95
GLO10	0.989	0	0.011	0	–1.25	–1.41
AG1	0.960	0.031	0	0.009	–0.90	–1.30
PERD	0.073	0	0.811	0.116	0.02	0.45
PERC	0.080	0	0.845	0.075	0.10	0.37
R2	0.127	0	0.873	0	0.46	–0.06
PM2	0.090	0	0.601	0.309	–0.36	0.45
ROM11	0.076	0	0.924	0	0.63	0.15
MBB	0.032	0	0.787	0.181	0.14	0.81
PER4	0.005	0	0.863	0.132	0.78	1.48
ROM9	0.025	0	0.964	0.011	0.94	0.58
MBA	0	0	0.843	0.157	0.53	1.24
ROM7	0	0	0.656	0.344	0.28	1.30
ROM4C	0	0	0.743	0.257	0.38	1.28
ROM3	0	0	0.110	0.890	–0.41	1.19
PER5	0	0	0.060	0.940	–0.57	1.11
<i>Teruel–Ademuz region, Teruel basin, Spain</i>						
CU	0.942	0	0.052	0.006	–0.75	–1.23
CASAL	0	0	0	1.000	–1.04	0.88
<i>Daroca region, Calatayud–Daroca basin, Spain</i>						
PED2C	0	0.573	0	0.427	0.28	1.28
PED2A	0	0.017	0.321	0.662	0.08	1.36
CAR1	0	0.465	0	0.535	0.16	1.28
NOM	0	0.042	0	0.958	–0.64	1.05
<i>Alicante, Spain</i>						
CR5	0.435	0.528	0.038	0	0.40	–0.45
CR4	0.346	0.342	0.312	0	0.88	–0.14

Table 5 (continued)

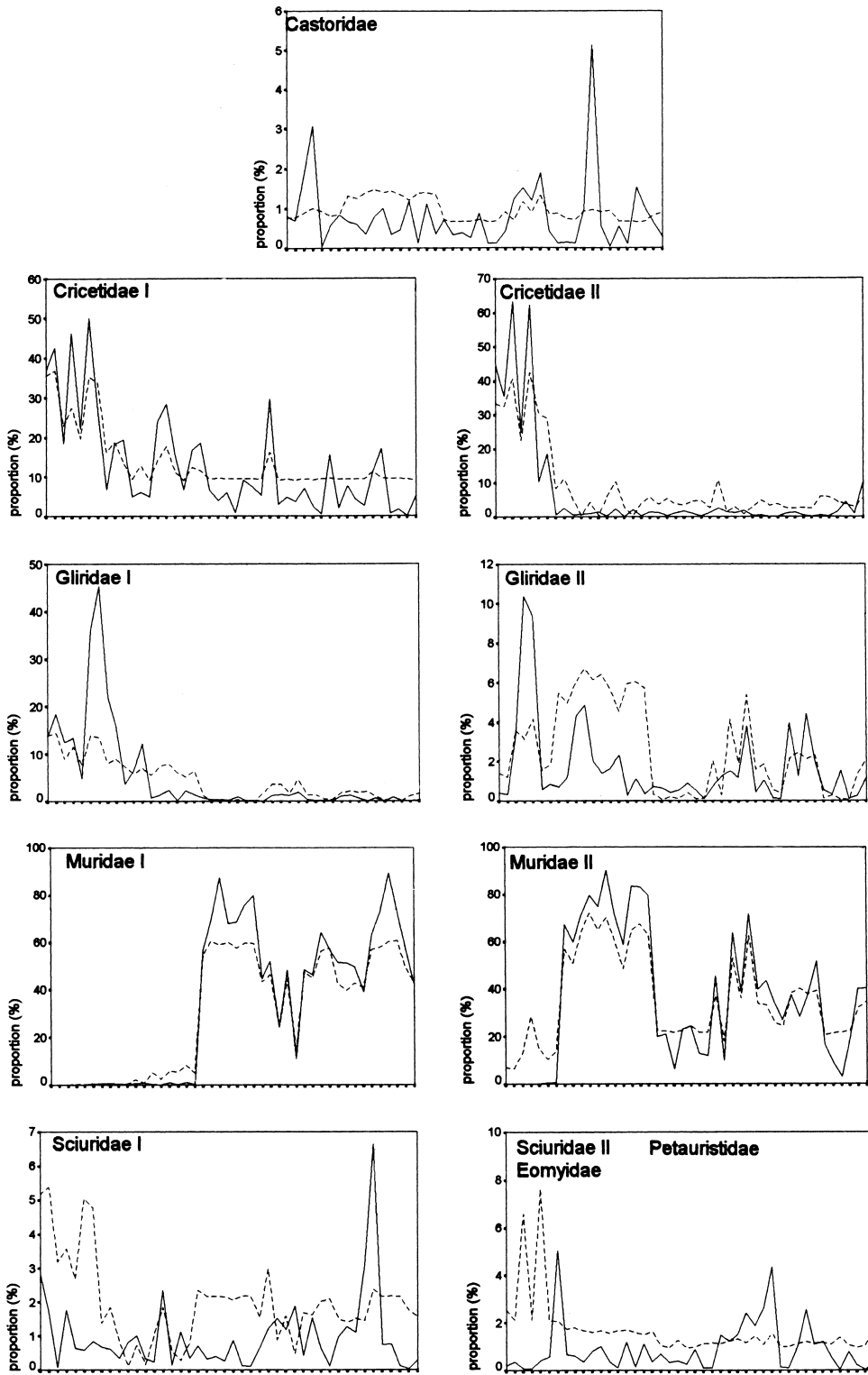
Locality	Contribution of end member (total = 1)				Climatic parameter (relative values)	
	1	2	3	4	humidity = –temperature	predictability = cool/warm seasonality = –wet/dry seasonality
CR3	0.720	0.186	0.094	0	0.20	–0.65
CR2	0.529	0.262	0.141	0.068	0.02	–0.20
CR1	0.588	0.250	0.162	0	0.48	–0.46
<i>Vallès-Penedès basin, Spain</i>						
TNA	0	1.000	0	0	1.33	0.88
TSA2	0	0.884	0	0.116	0.71	1.17
CL	0	0.824	0	0.774	0.59	1.21
CP	0.168	0	0	0.832	–1.82	–0.21
HSS	0.230	0	0	0.770	–1.89	–0.33
<i>Duero basin, Spain</i>						
TOR1	0.041	0.034	0.925	0	1.14	0.53
<i>Languedoc central, France</i>						
MONTR	0	0.884	0.009	0.107	0.70	1.14
<i>Cucuron–Basse Durance, France</i>						
CUCS	0.978	0.017	0	0.005	–0.96	–1.44
<i>Rhone basin/Lyon area, France</i>						
LS	0	0.126	0.874	0	1.89	1.21
DION	0.067	0.158	0.775	0	1.38	0.51
AMB3	0	1.000	0	0	1.33	0.88
AMB2	0	0.890	0.110	0	1.91	1.18
AMB1	0	0.497	0.503	0	2.13	1.31
SOBL	0.011	0.819	0.170	0	1.97	1.19
DOUVR	0.025	0.872	0.104	0	1.62	0.83
<i>Vienna basin, Austria</i>						
EICHK	0	0.666	0.334	0	2.11	1.29
<i>Strimon basin, Greece</i>						
PK4	0.170	0	0.611	0.219	–0.45	0.17
<i>Rafina basin, Greece</i>						
LEF	0.051	0.049	0.821	0.080	0.65	0.73

See Table 6 for estimation of climatic parameters.

which correspond to high differences in net scores in Table 4. Only differences larger than 2 are considered, and the maximum number of end-member pairs is set to four. For instance, the final humidity index is calculated as the first principal component of the four log-ratios corresponding to the end-member pairs 2–1, 2–4, 3–1 and 3–4. These pairs correspond to differences of 8, 11, 6 and 9, respectively (Table 6). It appears that the sets of pairs for humidity and temperature are identical, which implies that these two parameters are fully correlated. In other words they can be represented by a single signal, reflecting the variation between the two combinations cool–humid

and warm–arid. Table 6 also shows that seasonality type and predictability can be represented by a single signal, because two pairs with low net score differences can be omitted because of a negative loading on the first principal component. The resulting combinations are predictability and cool–warm seasonality on the one hand, and unpredictability and wet–dry seasonality on the other hand.

The final values of the climatic parameters for all localities are shown in Table 5. Fig. 9 shows the raw and smoothed values for the subset of localities from the CT basins. The combined humidity–temperature curve shows a long humid and cool phase between



~10.5–8.5 Ma, and shorter ones around 7 and 6 Ma. Two peaks (called small mammal (SM) events SM10A and SM12A in van Dam, 1997), occur at 9.4 and ~7 Ma. Arid and warm phases occur between 11.0 and 10.5, between 8.5 and 7.5 Ma and around 5 Ma. The seasonality–predictability signal shows a shift from a more predictable cool–warm seasonal climate to a more unpredictable wet–dry seasonal climate in two steps occurring at 9.4 to 9.0 and 8.7 to 8.2 Ma. The humidity–temperature and seasonality–predictability signals are strongly correlated ($r = 0.68$, $p < 0.001$ for all localities; $r = 0.64$, $p < 0.001$ for the CT basins). This means that the cooler and humid climates are also more cool–warm seasonal and more predictable. Fig. 9 shows that a main divergence between the two signals occurs in MN9 where relatively warm and dry conditions are combined with a relatively high predictability and strong cool–warm seasonality.

Fig. 10 shows palaeogeographic maps with mean parameter values per basin and MN zone. It should be stressed that some ‘mean’ values are based on one locality only, whereas others are based on many. Nevertheless, the figure shows some interesting patterns, such as a similarity between Spanish diagrams for MN10 (Fig. 10c) and the northern diagrams of both Fig. 10d,e (MN11–12). In some cases, strong similarities exist between areas from the same latitude and time slice, for instance Spain and Greece during MN10 and 12, and France and Austria during MN11. In addition, Fig. 10 shows climatic differences between coastal and continental areas. For example, the coastal Vallès-Penedès area scores higher on aridity and temperature, unpredictability and wet–dry seasonality than the CT area during early MN9 (Fig. 10a). During late MN9 and MN10 the situation is reversed with regard to humidity and temperature. Another example is Alicante (southern Spain), which shows somewhat higher humidities and lower average temperatures than the interiorly situated CT area during MN11–12.

The scatter diagram of Fig. 11 shows the inferred climatic features of all 67 localities. Three major and two minor clusters can be distinguished. The

transition from cluster 2 via cluster 3 to 4 reflects the general transition in Spain from a cool–warm seasonal, predictable climate during MN9–10 (cluster 2) towards a wet–dry seasonal and unpredictable climate in MN11–13 (cluster 4). The early MN9 localities, particularly HSS and CP from the Vallès-Penedès basin (cluster 1), fall outside the main trend. They are warm and dry, but with a relatively cool–warm seasonality. The northern localities EICHK from the Vienna basin and DOUVR, SOBL, AMB1–3, and DION from the Rhone area fall in the most humid–cool part of the diagram (in cluster 3). The northern MN11 localities (e.g. EICHK, AMB3, DION) are much more temperate than the contemporaneous Spanish localities. The three localities from the Teruel basin of cluster 5 differ climatically from the time-equivalent localities of cluster 4. Their aridity/temperature level is equal to that of cluster 1.

6.3. Robustness

Both the selection procedure for end-member pairs and the filtering effect of the principal component analysis (Table 6) contribute to the robustness of the method against errors in preferences and adaptations of groups in Table 2. Firstly, a change of a preference score does not necessarily lead to a different set of log-ratio pairs in Table 6, and secondly, if it does lead to another pair, PCA conservatively extracts the common signal shared by all logratios. Table 7 shows an example of this robustness: various alternatives for preferences and adaptations of Cricetidae result in identical sets of end-member pairs.

A second type of robustness relates to the sensitivity of climatic interpretations to structural under- or over-representation of groups. As an example, in Table 8 we check robustness against systematic demographic bias in gradually accumulating assemblages caused by differences in life expectancies of groups (Van Valen, 1964; Damuth, 1982). (The same reasoning applies to robustness against systematic taphonomic bias.) Correction factors are only approximate and represent typical life expectancy val-

Fig. 8. Comparison between model input (continuous line) and output (dashed line) for the nine environmental groups for the Calatayud–Daroca and Teruel basins. The x -axes represent localities from old (left) to young (right). Note the different scales on the y -axes.

Table 6
Selection procedure for sets of end-member pairs for each climatic parameter

Humidity	Temperature		Seasonality type (preparatory step 1)		Seasonality type/predictability	
	selected pair (net score difference Table 4)	loading on PC1 (43.5% explained)	selected pair (net score difference Table 4)	loading on PC1 (46.7% explained)	selected pair (net score difference Table 4)	loading on PC1 (74.9% explained)
2-1 (8)	0.77	1-2 (6)	2-1 (6)	0.78	2-1 (6/4)	0.75
2-4 (11)	0.61	1-3 (5)	2-4 (3)	-0.27	3-1 (6/3)	0.71
3-1 (6)	0.74	4-2 (7)	3-1 (6)	0.71	4-1 (3/5)	0.79
3-4 (9)	0.48	4-3 (6)	3-4 (3)	-0.42		
			4-1 (3)	0.98		

The choice of an initial set is made as follows: first, those end-member pairs are selected which correspond to complementary states in Table 4 (e.g. cooler vs. warmer). Next, those pairs are selected which correspond to a net score difference larger than 2 (numbers between brackets), with a maximum of four pairs (or more in the case of ex-aequo values). Finally, the log-ratios of end-member contributions are calculated according to Eq. 7, and used in a principal component analysis. The first component (PC1) is considered as the best estimator of the climatic parameter. Loadings of the log-ratios on the PC1s are shown. The procedure results in identical sets of pairs for humidity and temperature (first and third column). In the case of seasonality type, negative loadings on PC1 of pairs 2-4 and 3-4 appear (sixth column). Omission of these pairs yields the same set as selected for predictability (seventh column).

ues for demographic types after French et al. (1975). Corrected end-member compositions are calculated by multiplication of the percentages by the correction factors and scaling to 100%. It appears that end-member compositions are very different from those in Table 4, but that row-wise comparisons result in identical +, -, and 0 scores for eight of the nine groups, except in one case (a shift from a negative to a neutral score for the contribution of Castoridae to end member 1). Therefore, it may be concluded that our method of climatic interpretation of end members is very robust against systematic under- or over-representation in general, even when correction factors differ by a factor of five.

7. Discussion of the results

7.1. Other palaeoclimatic records from the Mediterranean

Martin and Braga (1994) and Brachert et al. (1996) discuss the climatic significance of the vertical alternation of coral reefs and bryozoan/mollusc-dominated carbonate ramps in the Neogene basins of the Betic Cordillera (southern Spain) (Fig. 12f). Warm episodes characterized by reefs occurred during the latest Serravallian(?) to earliest Tortonian, the early late Tortonian, the early Messinian, and the latest Messinian. Cooler intervals characterized by the dominance of bryozoans and molluscs occurred during the rest of the early Tortonian (including a radiometrically dated interval of which the onset and end are dated at 9.6 and 8.6 Ma, respectively), the latest Tortonian to earliest Messinian, and the middle to late Messinian. These climatic inferences fit our climatic interpretations (Figs. 9 and 12c) fairly well. It is not impossible that their latest Serravallian(?)–earliest Tortonian reef phase corresponds to our earliest Vallesian warming around 11 Ma, but because the reef-associated highstand is supposed to precede a marked lowstand at ~11 Ma (Fig. 12g) this correlation remains questionable.

Clay-mineral records from Sicily show abundant smectite in the middle Tortonian and Messinian sediments (Chamley et al., 1986; de Visser, 1991). Unfortunately, age control for the Tortonian part is poor, due to the lack of a refined biozonation. Linear interpola-

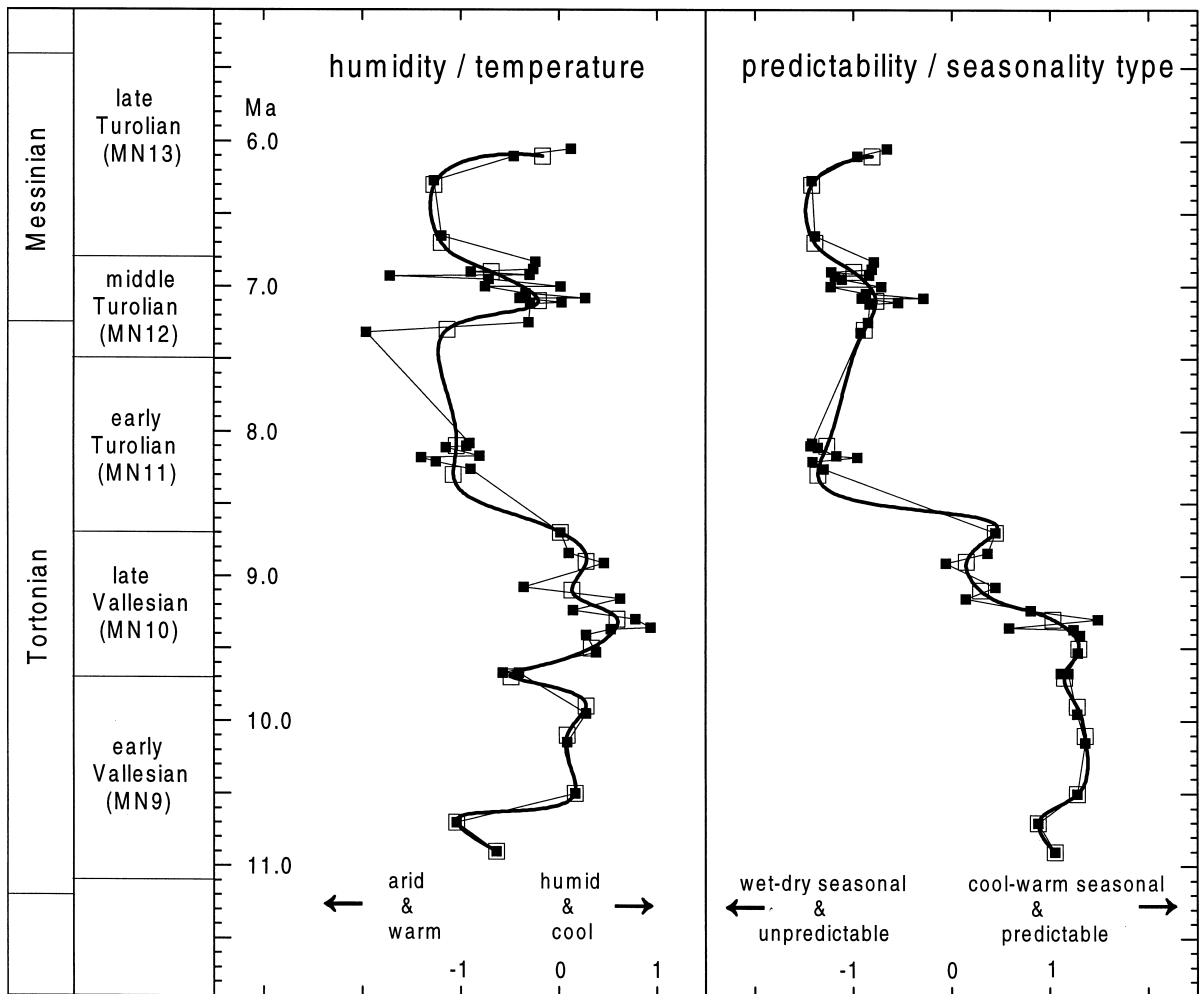


Fig. 9. Estimated climatic curves for the Calatayud–Daroca and Teruel basins relative to numerical time (ages converted to the scale of Cande and Kent, 1995). For locality ages see Table 1. The climatic parameters are expressed in relative values. Humidity and temperature are represented by a single signal. Likewise are predictability (= between-year variation) and seasonality type (= temperature vs. humidity-related seasonality). Thin lines with closed squares: raw estimates (Table 5). Thick lines: splined curves (spline tension factor 1) based on 17 time-averaged values (open squares, values for fixed time-intervals of 200 ka, with missing data at 10.3, 8.5, 7.9, 7.7, 7.5 and 6.5 Ma).

tion between two calibration points (*Neogloboquad-*
rina coiling change at 9.24 Ma, and the Tortonian–
Messinian boundary at 7.12 Ma, Krijgsman et al.,
1994a, 1995) results in an age of 9.0 Ma for the
onset of a gradual smectite increase, culminating in a
marked spike at 8.5–8.3 Ma. According to de Visser
(1991), this smectite increase may be attributed to
various processes, one of which is the development of a
warm climate with strong seasonal contrasts in
humidity. Other possibilities are rejuvenation of relief,

regression, and marine authigenesis. If the climatic
hypothesis is true, then the timing and interpretation
are strikingly similar to that based on our rodents,
which indicate warming and increasing wet–dry
seasonality between 9.4 and 8.2 Ma, with a maximum
occurring at ~8.3 Ma. Unfortunately, data for the
interval 8.0–7.5 Ma can not be compared because of a
gap in the Spanish rodent record.

A second smectite increase starts at about the
Tortonian–Messinian transition and continues well

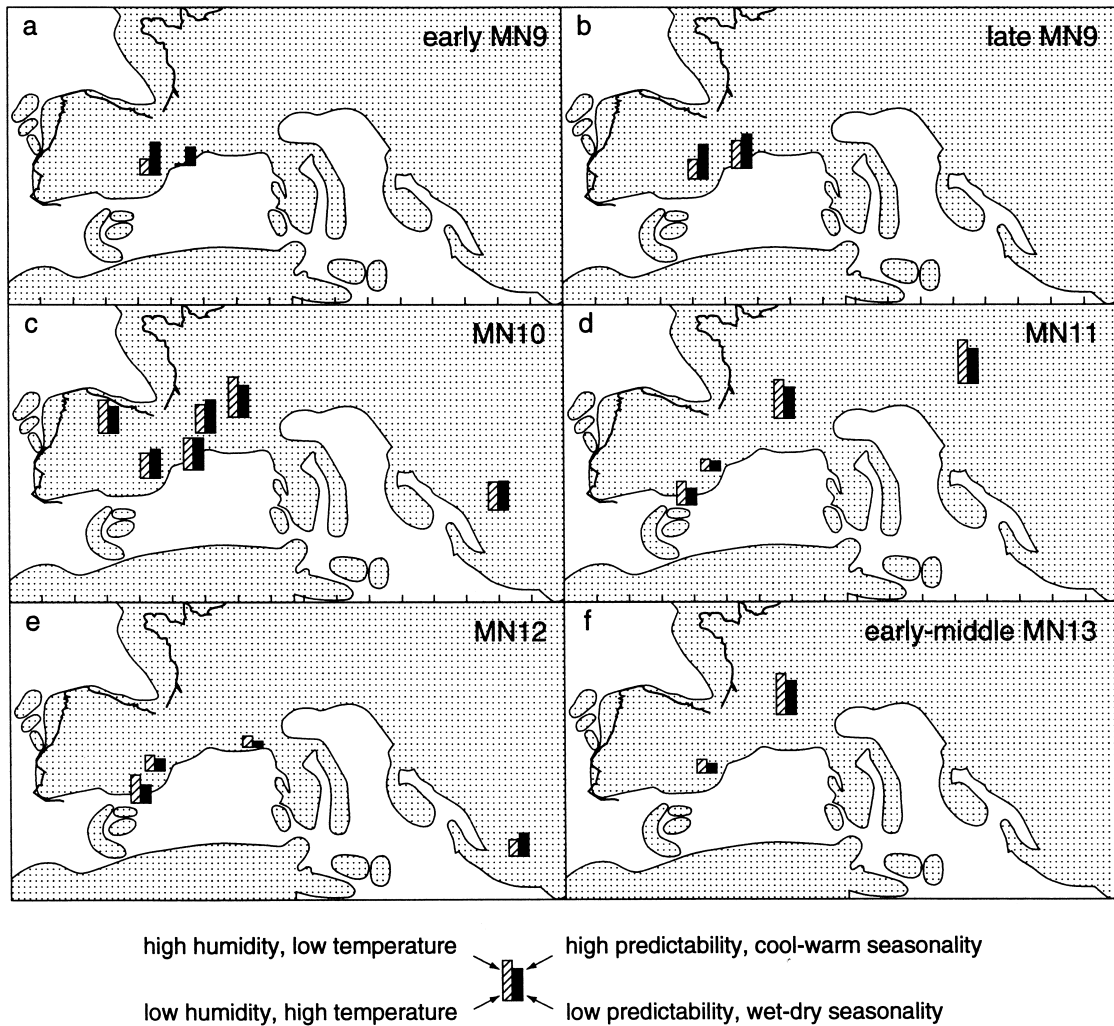


Fig. 10. Mean values for the relative humidity/temperature, and seasonality/predictability parameter per basin and zone. Note that some values are based on one locality only, whereas others are based on more. 'Early' MN9 localities are NOM, CASAL, CAR1, HSS and CP. Palaeogeographic basemap for the Tortonian after Dercourt et al. (1993).

into the Messinian. This rise correlates less well with our interpretation of the Spanish record. This record shows a maximum of warm and wet-dry seasonal conditions in a more restricted interval between 6.8 and 6.3 Ma (Fig. 9). No comparison can be made for the interval after 6 Ma because we have no rodent data covering this time slice.

Oxygen isotope values of planktonic foraminifera from sections on Sicily (van der Zwaan and Gudjonsson, 1986) do not show important trends or excursions over the studied interval. The carbon iso-

tope record, however, shows a marked shift towards lighter values between ~ 8.3 and 7.1 Ma. According to van der Zwaan and Gudjonsson (1986), this shift could correlate to the Late Miocene carbon shift as recognized in all major oceans (Keigwin and Shackleton, 1980; Vincent et al., 1980) between ~ 7.5 and 6.5 Ma, although the earlier start and larger amplitude of the Mediterranean shift is not well understood. Interesting are recent suggestions (Cerling et al., 1993; Hodell et al., 1994) for a relation between the global marine $\delta^{13}\text{C}$ shift and an opposite shift in

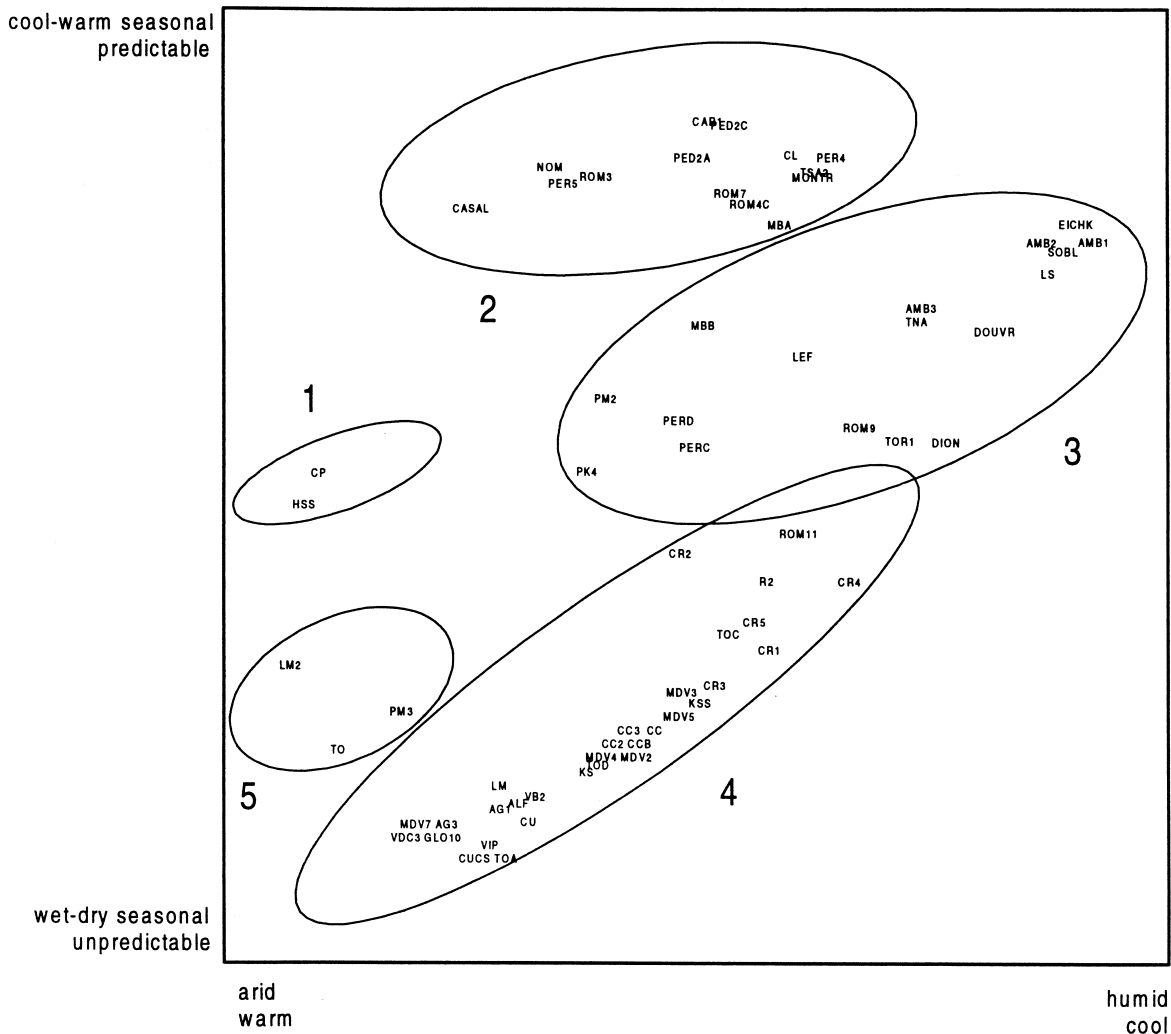


Fig. 11. Scatter diagram with positions of all 67 localities. Three major and two minor clusters can be distinguished. The transition from cluster 2 via cluster 3 to 4 reflects the general transition in Spain from a cool–warm seasonal, predictable climate during MN9–10 (cluster 2) towards a wet–dry seasonal and unpredictable climate in MN11–13 (cluster 4). The early MN9 localities, particularly HSS and CP from the Vallès-Penedès basin (cluster 1), fall outside the main trend. They are warm and dry, but relatively cool–warm seasonal. The northern localities EICHK from the Vienna basin and DOUVR, SOBL, AMB1–3, and DION from the Rhone area fall in the most humid–cool part of the diagram (in cluster 3). The northern MN11 localities (e.g. EICHK, AMB3, DION) are much more temperate than the contemporaneous Spanish localities. The three localities from the Teruel basin of cluster 5 differ climatically from the time-equivalent localities of cluster 4. Their aridity/temperature level is equal to that of cluster 1.

$\delta^{13}\text{C}$ as recorded in various terrestrial palaeosol and mammal enamel records across the world. Some of these records show an abrupt shift towards heavier isotopes between 7.5 and 6.5 Ma, whereas others show a more gradual shift between ~ 9 and ~ 6.5 Ma (Quade et al., 1989; Harrison et al., 1993; Morgan et al., 1994; Quade and Cerling, 1995). This terrestrial

shift, which is interpreted as a (global) replacement of C3 plants (trees, shrubs and cool-growing season grasses) by C4 plants (warm-growing season grasses), is not observed in a carbon isotope record from Greece. This record indicates a continuation of C3 vegetation, in the form of dry forest and woodland in a regime of winter or mixed-seasonal rain

Table 7

Robustness of climatic parameter estimation against alternative choices for preferences and adaptations of Cricetidae

Parameter and group	Score	Net score of all groups on end members				Resulting end-member pairs
		end m. 1	end m. 2	end m. 3	end m. 4	
Humidity (Cricetidae I)	0	−2	+6	+4	−5	2–1, 2–4, 3–1, 3–4
	−	−1	+5	+5	−6	2–1, 2–4, 3–1, 3–4
Temperature (Cricetidae I)	0	+3	−3	−2	+4	1–2, 1–3, 4–2, 4–3
	−	+4	−4	−1	+3	1–2, 1–3, 4–2, 4–3
	+	+2	−2	−3	+5	1–2, 1–3, 4–2, 4–3
Seasonality type (Cricetidae I)	0	−3	+3	+3	0	2–1, 3–1, 4–1, (2–4, 3–4)
	+	−4	+4	+2	+1	2–1, 3–1, 4–1, (2–4)
Seasonality type (Cricetidae I and II)	+	−5	+3	+1	+2	2–1, 3–1, 4–1

0 scores are from Table 2, + and − scores are alternatives. Net score calculation as in Table 4. End-member pair selection and PC1 calculation as in Table 6. Pairs between brackets can be omitted because of negative loadings on PC1. Alternatives result in identical sets of end-member pairs and hence in identical climatic parameter estimations.

Table 8

Robustness of climatic parameter estimation against structural under- or over-representation of groups

Group	Correction factor	Corrected end members (%)			
		1	2	3	4
Castoridae	9.95	2.89	3.61	4.63	1.59
Cricetidae I	3.35	13.64	7.72	9.41	25.62
Cricetidae II	3.35	5.44	56.99	0.00	22.64
Gliridae I	9.95	0.00	8.23	18.41	29.70
Gliridae II	9.95	0.00	22.93	21.26	2.49
Muridae I	1.80	47.50	0.27	0.43	0.00
Muridae II	1.80	16.93	7.18	41.19	2.44
Sciuridae I	9.95	9.46	2.35	0.00	11.08
Sciuridae II and Petauristidae and Eomyidae	9.95	4.06	39.47	4.94	4.43
Total		100.00	100.00	100.00	100.00

The effect of demographic bias is tested by a posterior correction of end-member compositions from Table 4. Correction factors are based on French et al. (1975) and represent mid-points of ranges of life-expectancy values for demographic groups. Only in one case (the proportion Castoridae in end member 1) row-wise comparison of proportions leads to scores different from those in Table 4.

(Quade et al., 1994). Given these results, it is not unreasonable to suggest that the shift towards more arid and wet–dry seasonal conditions as we inferred from the Spanish record between 9.4 and 8.2 Ma, is more related to summer than to winter dryness.

7.2. North–south gradients

Our reconstruction of a wetter and climatically more predictable zone (central Europe) north of a more arid and unpredictable zone (Spain and probably also Greece), is confirmed by an analysis of diversity. We counted the number of common rodent

genera in our data set covering the Late Miocene, which is the number of genera after counting 95% of the specimens, with the genera ranked from the most to the least abundant (Johnson, 1964). It appears that this number is about nine in the upper Vallesian–lower Turolian localities of the Rhone and Vienna basins, whereas in the CT basins in Spain it is only three on the average. Relations between climatic factors and diversity were studied by Slobodkin and Sanders (1969), who considered the diversity of a community as a function of the three environmental factors severity, variability and predictability. According to them the highest diversities occur in less

severe, and/or more predictable environments. According to Putman (1994, p. 125), a “temperate climax woodland with regular seasonal fluctuations” is an example of a favourable (= non-severe), variable and predictable terrestrial environment. Such type of environment probably corresponds to the central European part of our data set, which is characterized by large contributions of the end members 2 and 3.

Our model results seem to agree with reconstructions of Miocene vegetation zones (Wolfe, 1985; Tallis, 1991; Janis, 1993). These reconstructions point to a broad zone of temperate, broad-leaved deciduous woodlands or temperate seasonal forests north of a zone of sclerophyllous woodlands or Mediterranean shrublands. The latter zone becomes more distinct from the latest Middle Miocene onwards, when ‘Troekenfloren’ (dry floras) developed (Mai, 1995). Whether the distinction between the two vegetation belts also corresponds to a difference in climate types (*sensu* Köppen) is not sure. Macrofloral evidence from the Late Miocene of Europe points to the general presence of a Cfa climate (temperate–warm without a dry season), although also Cs and Cw climates (temperate–warm summer-dry and winter-dry, respectively) have been postulated for Mediterranean sites (review in Mai, 1995). The question whether the ‘mediterranean climate’, which is used as a synonym to a Cs climate by various authors, was already present in the Mediterranean area during the Late Miocene, seems partly to be a matter of definition (di Castri, 1981).

7.3. Low-frequency shifting of climate belts?

The next question is whether the long-term climatic fluctuations as observed for instance in Spain, are related to changes in the size and position of climate belts. Or more explicitly: do intervals of more humid–cooler conditions in Spain correspond to southward migrations of a Cfa climate and/or the associated seasonal forest or woodland zone?

Latitudinal migration of climate belts seems to be a common phenomenon on all time scales, resulting from changes in meridional thermal gradients and associated changes in the position of polar ice fronts and ocean surface temperatures. For example, precipitation zones shift seasonally, leading to a more southern position of the mid-latitude

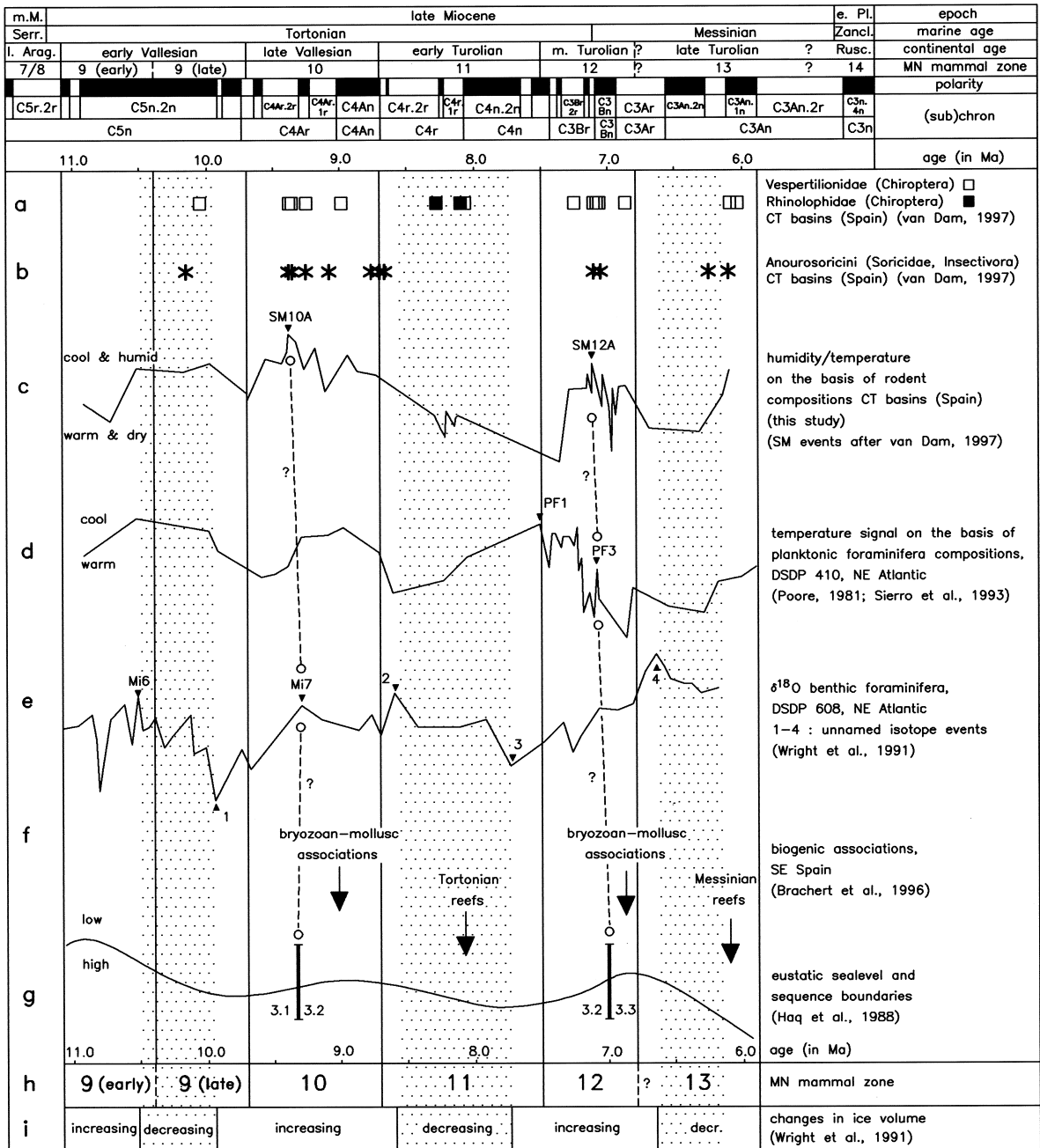
westerly winds and associated depressions during Northern Hemisphere winters. This southern migration of precipitation belts is assumed to occur also at the levels of decades (Agee, 1980), millennia (Lamb, 1972), and glacial maxima (e.g. Nicholson and Flohn, 1980). Variations in solar radiation at the scale of Milankovitch cycles are also expected to lead to circulation changes in about the same way, with polar cooling leading to the migration of zones and contraction of the Hadley cell (Perlmutter and Matthews, 1999). High-resolution records of marine flora and fauna indicate that astronomical forcing leads to migrational patterns with Milankovitch periodicities of ~20, 40, and 100 m.y. (Hays et al., 1976; Ruddiman and McIntyre, 1984; Beaufort and Aubry, 1990; Lourens et al., 1992) and their low-frequency modulations of 1.2 and 2.3 m.y. (Beaufort, 1994; Lourens and Hilgen, 1997).

Whether these types of low-frequency fluctuations also underlie or trigger the million-year scale variations in humidity and temperature as inferred for the Late Miocene of Spain is difficult to test with our data alone, because of the small number of areas per time slice. At best the Fig. 11c,e seem to indicate similar climatic trends in Spain, southernmost France, and Greece between MN10 and MN12. Furthermore, persistence of cooler and more humid climatic conditions in the Rhone area between MN10 and 13 (Fig. 10c–f) suggest that the boundary with the subtropical Mediterranean zone remained south of this area during that interval. Clearly, more data are needed to test the hypothesis of latitudinal shifting.

Insectivores were not included in our quantitative analyses. Nevertheless, some interesting examples of north–south migrations seem to confirm the results based on rodents. For instance, the intermittent presence of Anourosoricini (Soricidae, Insectivora) in the CT basins (Fig. 12b) corresponds fairly well with peaks of more humid and cool conditions (Fig. 12c). The presence of Anourosoricini in Spain during more temperate intervals can be seen as the result of occasional southward expansions, given the generally northern distribution of this tribe across Eurasia during the Neogene (Bachmayer and Wilson, 1970; Franzen and Storch, 1975; Storch and Zazhigin, 1996). A second example relates to the gradual southward migration of the Crocidosoricinae

from central to southern Europe during the Early to early Late Miocene, followed by their final extinction. These events were attributed to general cooling by Reumer (1994). New data from the Teruel basin (van Dam, 1997) show that the group disappeared

from this area around the late Vallesian temperature minimum. Possibly, the sparse Chiroptera (bat) record from the CT basins (Fig. 12a) is also a reflection of north–south migrations: Rhinolophidae are restricted to the early Turolian (MN11), which is a



warm interval according to the rodent-based model (Fig. 12c). Today this family of bats mainly lives in tropical zones. Open squares represent Vespertilionidae, a group which presently occur worldwide. Their clustering in MN10 and MN12/13 assemblages seems to confirm the lower temperatures during these intervals.

A scenario of latitudinal migration of climatic belts is advocated by Pickford and Morales (1994) who present a zoogeographic model based on ranges of Neogene macromammals from Spain and East Africa. These authors suggest that north–south shifts of the boundary zone between the ‘Paleo-Palaeartic’ and ‘Paleo-Ethiopian’ zoogeographic regions either opened or blocked critical passages through the Middle East and Afghanistan. During some intervals Spain would more belong to the ‘Paleo-Palaeartic’ region (for the Late Miocene this applies to MN9, MN10 and MN12), whereas during others it would belong to the ‘Paleo-Ethiopian’ region (early MN9, MN11, MN13). These results fit our rodent-based results very well except for MN13, for which the authors suggest a very northern position of their boundary (i.e. warm conditions). At least part of the lack of correspondence for MN13 may be explained by the absence of early MN13 macromammal localities in the data set of Pickford and Morales, and the absence of late MN13 micromammal localities in our data set.

If such low-frequency migrations of belts occurred, then their effects are expected to show up in oceanic records from the same latitude and region. Fig. 12c shows our humidity/temperature curve for Spain, which is compared to a principal component curve (Fig. 12d) based on planktonic foraminiferal abundances from DSDP Site 410 from the NE At-

lantic (Poore, 1981; Sierro et al., 1993), a benthic $\delta^{18}\text{O}$ curve (Fig. 12e) from DSDP site 608, NE Atlantic (Wright et al., 1991), and the eustatic sea-level curve (Fig. 12g) after Haq et al. (1988). The foraminiferal signal is supposed to indicate long-term cycles in sea surface temperature (Poore, 1981), while the oxygen isotope signal from site 608 has been interpreted in terms of low-frequency glacial–interglacial cycles (the stippled areas and Fig. 12i). Assuming that the sea-level signal is of glacio-eustatic origin, it may be expected to reflect glacial–interglacial cycles and, like curves d and e, to fit the scenario of shifting climate belts. The correspondence between the rodent and planktonic foraminiferal curve is fairly good. However, the correspondence between these two curves and the oxygen isotope curve is poor, especially after 8 Ma. The main differences between the sea-level curve and the rodent and foraminiferal curves concern the intervals before ~ 10.5 Ma and after ~ 6.5 Ma. The isotope and sea-level curves show a positive correlation, although low sea levels after 6.5 Ma correspond to an interval of relatively high $\delta^{18}\text{O}$ values. The alternation of coral reefs and bryozoan/mollusc-dominated associations (see above and Fig. 12f), of which the interpretation in terms of temperature fits well our results, is interpreted as the consequence of climate-controlled latitudinal shifting of the northern margins of the Miocene reef belt (Martin and Braga, 1994; Brachert et al., 1996). A general correlation of lower temperatures in Spain to sea-level lowstands (Fig. 12c.g) is also inferred by the latter authors, who correlate the warmer reef episodes to sea-level highstands and the cooler bryozoan/mollusc-dominated episodes to lowstands on the basis of the geometries and approximate datings of the various biogenic units (Fig. 12f.g).

Fig. 12. Various Late Miocene climate-related records, with a special emphasis on the NE Atlantic/W Mediterranean region. Solid vertical lines: continental age and mammal zone (MN) boundaries; ‘early’ and ‘late’ MN9 correspond to MN9 ‘a’ and ‘b’ of Agustí and Moyà-Sola (1991). Dashed lines: proposed correlations. Stippled areas: intervals of decreased ice volume according to Wright et al. (1991). Ages calibrated to the time scale of Cande and Kent (1995). The data for curve *d* were recalibrated by linear interpolation between five calibration points: base of chron C5r.1r (10.949 Ma), FAD of *Discoaster berggreni* (8.6 Ma; Berggren et al., 1996), planktonic foraminifer events PF1 (7.09 Ma) and PF3 (7.51 Ma) (ages according to Hodell et al., 1994), and Miocene–Pliocene boundary (5.3 Ma according to Berggren et al., 1996) which is regarded by Poore (1981) as equivalent to the highest unequivocal Miocene in core 410. The data for curve *e* were recalibrated by linear interpolation between ten calibration points: isotope events Mi6 (10.53 Ma) and Mi7 (9.31 Ma) (ages after Oslick et al., 1994, recalibrated to the Cande and Kent, 1995 time scale), chron boundaries C5An.1n–C5r.3r, C5r.1r–C5n.2n, C5n.1n–C4Ar.3r, C4Ar.2r–C4Ar.1n, C4Ar–C4r.2r, C4r.1r–C4n.2n, C4n.1n–C3Br.3r, and recalibration of age of core top (Wright et al., 1991: figs. 2 and 3). Range of absolute values for curve *e*: 1.77–2.37 parts per thousand. For curve *g* we used Haq et al. (1988) calibration to the geomagnetic polarity pattern. Range of sea level in curve *g*: ~ -50 to $+50$ m relative to the present-day level.

Both the rodent-based cooling peaks SM10A and SM12A are close in time to clusters of (related?) marine events. SM10A (9.4 Ma) correlates well with global oxygen-isotope event Mi7 (9.31 Ma) (Wright and Miller, 1992; age after Oslick et al., 1994) and to sequence boundary 3.1/3.2 (Haq et al., 1988). Sequence boundaries are generally thought to correlate with times of most rapid glacio-eustatic lowerings, and therefore to be stratigraphically close to Mi events (Miller et al., 1991). The clustering of events around 9.4–9.3 Ma could represent a climatic minimum within an early Late Miocene predominantly cool episode. Studies on Antarctic and Southern Ocean deep-sea cores indicate that the West Antarctic ice sheet probably started to develop by this time (Cieselski and Weaver, 1983; Robin, 1988; Kennett and Barker, 1990). Scattered ice build-up at Northern Hemisphere high latitudes around this time is indicated by ice-rafted debris (IRD) and glacier-related deposits (Denton and Armstrong, 1969; Hamilton, 1986; Schaeffer and Spiegler, 1986; Jansen et al., 1995; Wolf-Welling et al., 1995). Palynological data from Iceland indicate a strong cooling between 10 and 9.5 Ma (Mudie and Helgason, 1983), i.e. slightly before our maximum at 9.3–9.4 Ma.

Although alternative palaeomagnetic interpretations are possible for the middle to late Turolian sections in the CT basins (van Dam, 1997), the most probable solution points to an age around 7 Ma for cooling event SM12A, which is temporally close to sequence boundary 3.2/3.3 and close to the base of the Messinian (7.12 Ma, Krijgsman et al., 1994a, 1995) and planktonic foraminiferal cooling event PF3 (7.09 Ma, Sierro et al., 1993; Hodell et al., 1994). However, there is no oxygen isotope excursion analogous to Mi7 at Site 608 around 7.1 Ma, although Hodell et al. (1994) note a two-step increase in $\delta^{18}\text{O}$ around the Tortonian–Messinian transition in Morocco, the first of which occurs at 7.17 Ma. The general shift towards heavier isotopes, which is observed at various oceanic sites at this time, probably marks the onset of a latest Miocene (Messinian) phase of renewed glacial expansion on the Southern Hemisphere (Mercer, 1983; see also Cita and McKenzie, 1986). Supposedly, the West Antarctic ice sheet became a permanent, stable feature by then (Kennett, 1986; Kennett and Barker, 1990; Ehrmann et al., 1992). In addition, there is ev-

idence for scattered Northern Hemisphere glaciation at these times (Jansen and Sjøholm, 1991; Larsen et al., 1994; Wolf-Welling et al., 1995). The lack of correspondence between the curves of Fig. 12 for the interval after ~ 8 Ma may be indicative of the complex relation between ice accumulation and temperature at Northern Hemisphere mid-latitudes. The apparent lack of correspondence between polar and Mediterranean cooling during the Messinian is perhaps not surprising, because of the high probability of a regional climatic overprint in the Mediterranean in connection with the salinity crisis.

Lourens and Hilgen (1997) correlate Plio–Pleistocene third-order sea-level cycles to astronomical cycles, in particular to a low-frequency (1.2 m.y.) modulation of the 41,000 year earth obliquity signal. However, they note that such correlations work less well for the Middle to Late Miocene, where a modulation of the $\sim 100,000$ year eccentricity signal with a periodicity of 2.3 m.y. seems to be more pronounced. This 2.3 m.y. signal is recognized in sapropel patterns (Hilgen et al., 1995) and planktonic foraminiferal abundances (Lourens and Hilgen, 1997). The % left-coiling neogloboquadrinids (from 10 to 6.6 Ma), used by the latter authors as a low-temperature proxy, indicates warmings at 10–9.5 and 7.7–7.3 Ma, together bracketing one complete cycle of ~ 2.3 m.y. Cooler conditions occur between 9.4 and 8.4 Ma and 6.8 and 6.6 Ma. The temperature signal corresponds more or less to our temperature signal for Spain, except for the latter cooling (Fig. 9). It is interesting that our interval of most marked faunal and climatic turnover (9.0 to 8.3 Ma) around the Vallesian–Turolian boundary (8.7 Ma) is close in time to an interval of strong oscillations in neogloboquadrinids between 8.7–8.3 Ma. These oscillations would indicate a cooling maximum at 8.7 Ma, followed by a warming maximum at 8.5 Ma, which is immediately followed by a strong cooling at 8.4 Ma and a more permanent return to warmer conditions at 8.3 Ma. Indirect links between long-term astronomical forcing and changes in terrestrial ecosystems, if existing, will undoubtedly be complex. More long, detailed, and dated time series from different areas are needed to be able to demonstrate the reality and nature of such relations.

8. Conclusions

The main conclusions are the following.

(1) End-member modelling is a useful method to extract palaeoclimatic information from series of fossil rodent assemblages. The specific bilinear unmixing solution used here yields well-interpretable sets of end members. The contributions of these members to the samples can easily be converted to relative values for climatic parameters, given the preferences and adaptations of the rodent groups.

(2) Life-history characteristics deserve to be used more in small-mammal based palaeoecological and -climatological reconstructions, because they carry valuable information on the seasonal aspects of climate.

(3) The model results for Spain indicate more humid and cooler conditions between 10.5 and 8.5, around 7, and around 6 Ma, and more arid and warmer conditions prior to 10.5, between 8.6 and 7.5 Ma and around 6.5 Ma. Superimposed on this pattern is a shift from a more predictable, cool–warm seasonal climate towards a more unpredictable, wet–dry seasonal climate between 9.4 and 8.2 Ma. A fairly abrupt transition existed between a southern and northern climate zone in Europe during at least a part of the studied interval. The southern climate is dryer, warmer, more wet–dry seasonal and more unpredictable than the northern one.

Acknowledgements

We thank Hans de Bruijn, John Damuth, Frits Hilgen, Johan Meulenkamp, Albert van der Meulen, Jelle Reumer, Jan Willem Zachariasse and Bert van der Zwaan for their suggestions and critical reading of the manuscript. We thank the journal reviewers for constructive comments. We thank Prof. Dr. C.J.E. Schuurmans for discussing the subject of topographic effects on atmospheric circulation. We are grateful to Jacco van Bergenhenegouwen, Tom van Hinte and Jaap Luteyn for preparing various figures. Gert Jan Weltje was financed by the Geosciences Foundation (GOA) of the Netherlands Organization for Scientific Research (NWO). This publication is No. 990104 of the Netherlands Research School of Sedimentary Geology (NSG).

References

- Agee, E.M., 1980. Present climatic cooling and a proposed causative mechanism. *Bull. Am. Meteorol. Soc.* 61, 1356–1367.
- Aguilar, J.-P., Michaux, J., 1990. A paleoenvironmental and paleoclimatic interpretation of a Miocene rodent faunal succession in southern France. Critical evaluation of the use of rodents in paleoecology. *Paléobiol. Continentale* 16, 311–327.
- Agustí, J., 1981. *Roedores miomorfos del Neógeno de Catalunya*. Ph.D. Thesis, University of Barcelona.
- Agustí, J., 1990. The Miocene rodent succession in eastern Spain: a zoogeographical appraisal. In: Lindsay, E.H., Fahlbusch, V., Mein, P. (Eds.), *European Neogene Mammal Chronology*. Plenum, New York, pp. 375–404.
- Agustí, J., Gibert, J., 1982a. *Roedores e insectívoros del Mioceno Superior dels Hostalets de Pierola (Vallès-Penedès, Catalunya)*. *Butlletí Informatiu, Institut de Paleontologia de Sabadell* 14, 19–37.
- Agustí, J., Gibert, J., 1982b. *Roedores e insectívoros (Mammalia) del Mioceno Superior de Can Jofresa y Can Perellada (Vallès-Penedès, Catalunya)*. *Paleontol. Evoluc.* 17, 29–41.
- Agustí, J., Moyà-Sola, S., 1991. Spanish Neogene mammal succession and its bearing on continental biochronology. *Newslet. Stratigr.* 25, 91–114.
- Aitchison, J., 1986. *The Statistical Analysis of Compositional Data*. Chapman and Hall, London.
- Alvarez Sierra, M.A., 1983. *Paleontología y bioestratigrafía del Mioceno superior del sector central de la Cuenca del Duero: Estudio de los micromamíferos de la Serie de Torremormojón (Palencia)*. Ph.D. Tesis de Licenciatura, Complutense University Madrid.
- Alvarez Sierra, M.A., 1987. *Estudio sistemático y bioestratigráfico de los Eomyidae (Rodentia, Mammalia) del Oligoceno superior y Mioceno inferior español*. *Scripta Geol.* 86, 1–207.
- Axelrod, D.I., Bailey, H.P., 1969. Paleotemperature analysis of Tertiary floras. *Palaeogeogr., Palaeoclimatol., Palaeoecol.* 6, 163–195.
- Bachmayer, F., Wilson, R.W., 1970. Die Fauna der altplioziänen Höhlen- und Spalten-füllungen bei Kohfidisch, Burgenland (Österreich). *Ann. Naturhist. Mus. Wien* 74, 533–587.
- Badgley, C.E., Behrensmeyer, K.A., 1995. Preservation, paleoecological and evolutionary patterns in the Wyoming–Montana Paleogene and Siwalik Neogene fossil records. *Palaeogeogr., Palaeoclimatol., Palaeoecol.* 115, 1–11.
- Barron, E.J., 1985. Explanations of the Tertiary global cooling trend. *Palaeogeogr., Palaeoclimatol., Palaeoecol.* 50, 45–61.
- Barry, J.C., Flynn, L.J., Pilbeam, D.R., 1990. Faunal diversity and turnover in a Miocene terrestrial sequence. In: Ross, R., Allmon, W. (Eds.), *Causes of Evolution: A Paleontological Perspective*. University of Chicago Press, Chicago, pp. 381–421.
- Beaufort, L., 1994. Climate importance of the modulation of the 100 kyr cycle inferred from 16 m.y. long Miocene records. *Paleoceanography* 9, 821–834.
- Beaufort, L., Aubry, M.-P., 1990. Fluctuations in the composi-

- tion of late Miocene calcareous nannofossil assemblages as a response to orbital forcing. *Paleoceanography* 5, 845–865.
- Berggren, W.A., Kent, D.V., Swisher, C.C., III, Aubry, M., 1996. A revised Cenozoic geochronology and chronostratigraphy. *Soc. Econ. Paleontol. Mineral. Spec. Vol.*, 54: 129–212.
- Besems, R.E., van de Weerd, A., 1983. The Neogene rodent biostratigraphy of the Teruel-Ademuz Basin (Spain). *Proc. K. Ned. Acad. Wet. B* 86, 17–24.
- Bezdek, J.C., Ehrlich, R., Full, W.E., 1984. FCM: the fuzzy c-means clustering algorithm. *Comput. Geosci.* 19, 191–204.
- Birks, H.J.B., 1985. Recent and possible future mathematical developments in quantitative palaeoecology. *Palaeogeogr., Palaeoclimatol., Palaeoecol.* 50, 107–147.
- Bolliger, T., 1992. Kleinsäugerstratigraphie in der miozänen Hörnlichschüttung (Ostschweiz). *Doc. Naturae* 75, 1–296.
- Brachert, T.C., Betzler, C., Braga, J.C., Martin, J.M., 1996. Record of climatic change in neritic carbonates: turnover in biogenic associations and depositional modes (Late Miocene, southern Spain). *Geol. Rundsch.* 85, 327–337.
- Burchard, B., 1978. Oxygen isotope paleotemperatures from the Tertiary period in the North Sea area. *Nature* 275, 121–123.
- Cade, T.J., 1964. The evolution of torpidity in rodents. *Ann. Acad. Sci. Fenn. Ser. A, IV. Biol.* 71, 77–112.
- Cande, S.C., Kent, D.K., 1995. Revised calibration of the geomagnetic polarity time scale for the Late Cretaceous and Cenozoic. *J. Geophys. Res.* 100, 6093–6095.
- Cerling, T.E., Wang, Y., Quade, J., 1993. Expansion of C4 ecosystems as an indicator of global ecological change in the Late Miocene. *Nature* 361, 344–345.
- Chaline, J., Mein, P., Petter, F., 1977. Les grandes lignes d'une classification évolutive des Muroidea. *Mammalia* 41, 245–251.
- Chamley, H., Meulenkamp, J.E., Zachariasse, W.J., van der Zwaan, G.J., 1986. Middle to Late Miocene marine ecotratigraphy: clay minerals, planctonic foraminifera and stable isotopes from Sicily. *Oceanol. Acta* 9, 227–238.
- Cieselski, P.F., Weaver, F.M., 1983. Neogene and Quaternary paleoenvironmental history of Deep Sea Drilling Project Leg 171 sediments: southwest Atlantic Ocean. *Init. Rep. DSDP* 71, 461–477.
- Cita, M.B., McKenzie, J.A., 1986. The terminal Miocene event. *Geodyn.* 15, 123–140.
- Coiffait, B., 1991. Contribution des rongeurs du Neogène d'Algérie à la biochronologie mammalienne d'Afrique nord-occidentale. Ph.D. Thesis, Nancy.
- Daams, R., de Bruijn, H., 1995. A classification of the Gliridae (Rodentia) on the basis of dental morphology. *Hystrix* 6, 3–35.
- Daams, R., van der Meulen, A.J., 1984. Paleoenvironmental and paleoclimatic interpretation of micromammal faunal successions in the Upper Oligocene and Miocene of north central Spain. *Paléobiol. Continentale* 14, 241–257.
- Daams, R., Freudenthal, M., van der Meulen, A.J., 1988. Ecotratigraphy of micromammal faunas from the Neogene of the Calatayud–Teruel Basin. *Scripta Geol. Spec. Iss.* 1, 287–302.
- Damuth, J., 1982. Analysis of the preservation of community structure in assemblages of fossil mammals. *Paleobiology* 8, 434–446.
- Daxner-Höck, G., 1980. Rodentia (Mammalia) des Eichkogels bei Mödling (Niederösterreich). *Ann. Naturhist. Mus. Wien* 83, 135–152.
- de Bruijn, H., 1976. Vallesian and Turolian rodents from Biota: Attica and Rhodes (Greece). *Proc. K. Ned. Acad. Wet. B* 79, 361–384.
- de Bruijn, H., 1989. Smaller mammals from the Upper Miocene and Lower Pliocene of the Strimon Basin, Greece, Part 1. Rodentia and Lagomorpha. *Boll. Soc. Paleontol. Ital.* 28, 189–195.
- de Bruijn, H., 1995. The vertebrate locality Maramena (Macedonia, Greece) at the Turolian–Ruscian boundary 8: Sciuridae, Petauristidae and Eomyidae (Rodentia, Mammalia). *Münchner Geowiss. Abh. A* 28, 87–102.
- de Bruijn, H., Mein, P., Montenat, C., van de Weerd, A., 1975. Correlations entre les gisements de rongeurs et les formations marines du Miocène terminal d'Espagne meridionale (provinces d'Alicante et de Murcia). *Proc. K. Ned. Acad. Wet. B* 78, 1–32.
- de Bruijn, H., Daams, R., Daxner-Höck, G., Fahlbusch, V., Ginsburg, L., Mein, P., Morales, J., 1992. Report of the RCMNS working group on fossil mammals, Reisenburg 1990. *Newsl. Stratigr.* 26, 65–118.
- de Bruijn, H., Fahlbusch, V., Saraç, C., Ünay, E., 1993. Early Miocene rodent faunas from the eastern Mediterranean area. Part III. The genera *Deperetomys* and *Cricetodon* with a discussion of the evolutionary history of the Cricetodontini. *Proc. K. Ned. Acad. Wet. B* 96, 151–216.
- de Bruijn, H., van Dam, J.A., Daxner-Höck G., Fahlbusch V., Storch G., 1996. The genera of Murinae endemic insular forms excepted of Europe and Anatolia during the Late Miocene and Early Pliocene. In: Bernor, R.L., Fahlbusch, V., Mittmann, H.-W. (Eds.), *The Evolution of Western Eurasian Neogene Mammal Faunas*. Columbia University Press, New York, pp. 253–260.
- Denton, G.H., Armstrong, R.L., 1969. Miocene–Pliocene glaciations in Southern Alaska. *Am. J. Sci.* 267, 1121–1142.
- Dercourt, J., Ricou, L.E., Vrielynck, B., 1993. Atlas Tethys Paleoenvironmental Maps. Gauthier-Villars, Paris.
- de Visser, J.P., 1991. Clay mineral stratigraphy of Miocene to recent marine sediments in the central Mediterranean. *Geol. Ultraiectina* 75, 1–244.
- di Castri, F., 1981. Mediterranean-type of shrublands of the world. In: di Castri, F., Goodall, D.W., Specht, R.L. (Eds.), *Mediterranean-Type Shrublands. Ecosystems of the World* 11, Elsevier, Amsterdam, pp. 1–52.
- Ehrmann, W.U., Hambrey, M.J., Baldauf, J.G., Barron, J., Larsen, B., Mackensen, A., Wise Jr., S.W., Zachos, J.C., 1992. History of Antarctic glaciation: an Indian Ocean perspective. *Geophys. Monogr.* 70, 423–446.
- Engesser, B., 1990. Die Eomyidae (Rodentia, Mammalia) der Molasse der Schweiz und Savoyens. *Schweiz. Paläontol. Abh.* 112, 1–144.
- Fahlbusch, V., 1978. Pliozäne und Pleistozäne Eomyidae (Rodentia, Mammalia) aus Polen. *Acta Zool. Cracov.* 23, 13–26.
- Fahlbusch, V., 1979. Eomyidae — Geschichte einer Säugetierfamilie. *Paläontol. Z.* 53, 90–97.
- Fahlbusch, V., Bolliger, T., 1996. Eomyids and Zapodids (Roden-

- tia and Mammalia) in the Middle and Upper Miocene of Central and Southeastern Europe and the Eastern Mediterranean. In: Bernor, R.L., Fahlbusch, V., Mittmann, H.-W. (Eds.), *The Evolution of Western Eurasian Neogene Mammal Faunas*. Columbia University Press, New York, pp. 208–212.
- Flower, B.P., Kennett, J.P., 1993. Middle Miocene ocean-climate transition: High-resolution oxygen and carbon isotopic records from Deep Sea Drilling Project Site 588A: southwest Pacific. *Paleoceanography* 8, 811–843.
- Frakes, L.A., Francis, J.E., Syktus, J.I., 1992. *Climate Modes of the Phanerozoic*. Cambridge University Press, Cambridge.
- Franzen, J.L., Storch, G., 1975. Die unterpliozäne (turolische) Wirbeltierfauna von Dorn-Dürkheim, Rheinhessen (SW-Deutschland). *Senckenbergiana Lethaea* 56, 233–303.
- French, N.R., D.M. Stoddart, and B. Bobek, 1975. Patterns of demography in small mammal populations. In: Golley, F.B., Petruszewicz, K., Ryszkowski, L. (Eds.), *Small Mammals: Their Productivity and Population Dynamics*. Cambridge University Press, Cambridge, pp. 73–102.
- Freudenthal, M., Sondaar, P.Y., 1964. Les faunes à Hipparion des environs de Daroca (Espagne) et leur valeur pour la stratigraphie du Néogène de l'Europe. *Proc. K. Ned. Acad. Wet. B* 67, 473–490.
- Full, W.E., Ehrlich, R., Klován, J.E., 1981. Objective definition of external endmembers in the analysis of mixtures. *Math. Geol.* 13, 331–344.
- Full, W.E., Ehrlich, R., Bezdek, J.C., 1982. FUZZY QMODEL — a new approach for linear unmixing. *Math. Geol.* 14, 259–270.
- Garcés, M., Agustí, J., Cabrera, L., Parés, J.M., 1996. Magnetostratigraphy of the Vallesian (Late Miocene) in the Vallès-Penedès Basin (northeast Spain). *Earth Planet. Sci. Lett.* 142, 381–396.
- Garcés, M., Krijgsman, W., Dam, J. van, Calvo, J.P., Alcalá, L., Alonso-Zarza, A.M., 1999. Late Miocene alluvial sediments from the Teruel area: Magnetostratigraphy, magnetic susceptibility, and facies organisation. *Acta Geol. Hisp.* (in press).
- Giller, P.S., Gee, J.H.R., 1986. The analysis of community organization: the influence of equilibrium, scale and terminology. In: Gee, J.H.R., Giller, P.S. (Eds.), *Organization of Communities*. Blackwell, Oxford, pp. 519–542.
- Gotelli, N.J., Graves, G.R., 1996. *Null Models in Ecology*. Smithsonian Institution, Washington, D.C.
- Grant, P.R., 1972. Interspecific competition among rodents. *Annu. Rev. Ecol. Syst.* 3, 79–106.
- Gunnell, G.F., Morgan, M.E., Maas, M., Gingerich, P.D., 1995. Comparative paleoecology of Paleogene and Neogene mammalian faunas: trophic structure and composition. *Palaeogeogr., Palaeoclimatol., Palaeoecol.* 115, 265–286.
- Hamilton, T.D., 1986. Correlation of Quaternary glacial deposits in Alaska. *Quat. Sci. Rev.* 5, 171–180.
- Haq, B.U., Hardebol, J., Vail, P., 1988. Mesozoic and Cenozoic chronostratigraphy and cycles of sea-level change. *Soc. Econ. Paleontol. Mineral. Spec. Publ.* 42, 71–108.
- Harrison, T.M., Copeland, T., Hall, S.A., Quade, J., Burner, S., Oyha, T.P., Kidd, W.S.F., 1993. Isotopic preservation of Himalayan/Tibetan uplift, denudation, and climatic histories in two molasse deposits. *J. Geol.* 101, 157–175.
- Hays, J.D., Imbrie, J., Shackleton, N.J., 1976. Variations in the earth's orbit: pacemaker of the ice ages. *Science* 194, 1121–1132.
- Hilgen, F.J., Krijgsman, W., Langereis, C.G., Lourens, L.J., Santarelli, A., Zachariasse, W.J., 1995. Extending the astronomical (polarity) time scale into the Miocene. *Earth Planet. Sci. Lett.* 136, 495–510.
- Hodell, D.A., Woodruff, F., 1994. Variations in the strontium isotopic ratio of seawater during the Miocene: stratigraphic and geochemical implications. *Paleoceanography* 9, 405–426.
- Hodell, D.A., Benson, R.H., Kent, D.V., Boersma, A., Rakic-El Bied, K., 1994. Magnetostratigraphic, biostratigraphic and stable isotope stratigraphy of an Upper Miocene drill core from the Salé Briqueterie (northwestern Morocco): a high-resolution chronology for the Messinian stage. *Paleoceanography* 9, 835–855.
- Huguene, M., Mein, P., 1965. Lagomorphes et rongeurs du Néogène de Lissieu (Rhône). *Trav. Lab. Géol. Faculté Sci. Lyon* 12, 109–123.
- Jaeger, J.J., 1977. Les rongeurs du Miocène moyen et supérieur du Maghreb. *Palaeovertebrata* 8, 1–166.
- Janis, C.M., 1993. Tertiary mammal evolution in the context of changing climates, vegetation, and tectonic events. *Annu. Rev. Ecol. Syst.* 24, 467–500.
- Jansen, E., Sjøholm, J., 1991. Reconstruction of glaciation over the past 6 Myr from ice-born deposits in the Norwegian Sea. *Nature* 349, 600–603.
- Jansen, E., Fronval, T., Koç, N., 1995. Miocene to Recent paleoclimatic evolution at high Northern latitudes: interhemisphere linkages. *Abstr. Prog. 5th Int. Conf. Paleoceanogr. Halifax* 20.
- Johnson, R.G. 1964. The community approach to paleoecology. In: Imbrie, J., Newell, N. (Eds.), *Approaches to Paleocology*. Wiley, New York, pp. 107–134.
- Keigwin Jr., L.D., Shackleton, N.J., 1980. Uppermost Miocene carbon isotope stratigraphy of a piston core in the equatorial Pacific. *Nature* 284, 613–614.
- Kennett, J.P., 1986. Miocene to early Pliocene oxygen and carbon isotope stratigraphy in the southwest Pacific: Deep Sea Drilling Project Leg 90. *Init. Rep. DSDP 90*, 1383–1411.
- Kennett, J.P., Barker, P.F., 1990. Latest Cretaceous to Cenozoic climate and oceanographic developments in the Weddell Sea, Antarctica: an ocean-drilling perspective. *Proc. ODP Sci. Results* 113, 937–960.
- Kingdon, J., 1974. *East African mammals, Volume II, Part B. Hares and rodents*. University of Chicago Press, Chicago.
- Klován, J.E., Miesch, A.T., 1976. Extended CABFAC and QMODEL computer programs for Q-mode factor analysis of compositional data. *Comput. Geosci.* 22, 631–637.
- Korth, W.W., 1994. *The Tertiary Record of Rodents in North America*. Plenum Press, New York.
- Kowalski, K., 1990. Stratigraphy of Neogene mammals of Poland. In: Lindsay, E.H., Fahlbusch, V., Mein, P. (Eds.), *European Neogene Mammal Chronology*. Plenum, New York, pp. 193–210.
- Krijgsman, W., Hilgen, F.J., Langereis, C.G., Zachariasse, W.J.,

- 1994a. The age of the Tortonian/Messinian boundary. *Earth Planet. Sci. Lett.* 121, 533–547.
- Krijgsman, W., Langereis, C.G., Daams, R., van der Meulen, A.J., 1994b. Magnetostratigraphic dating of the Middle Miocene climatic change in the continental deposits of the Aragonian type area in the Calatayud–Teruel basin (Central Spain). *Earth Planet. Sci. Lett.* 128, 513–526.
- Krijgsman, W., Hilgen, F.J., Langereis, C.G., Santarelli, A., Zachariasse, W.J., 1995. Late Miocene magnetostratigraphy, biostratigraphy and cyclostratigraphy in the Mediterranean. *Earth Planet. Sci. Lett.* 136, 475–494.
- Krijgsman, W., Garcés, M., Langereis, C.G., Daams, R., van Dam, J., van der Meulen, A.J., Agustí, J., Cabrera, L., 1996. A new chronology for the middle to Late Miocene continental record in Spain. *Earth Planet. Sci. Lett.* 142, 367–380.
- Lamb, H.H., 1972. *Climate, Present, Past and Future*. Volume 1, Methuen, London.
- Larsen, H.C., Saunders, A.D., Clift, P.D., Beget, J., Wei, Spetzferri, W.S. and ODP Leg 152 Scientific Party, 1994. Seven million years of glaciation in Greenland. *Science* 264, 952–955.
- Lourens, L., Hilgen, F.J., 1997. Long-periodic variations in the earth's obliquity and their relation to third-order eustatic cycles and late Neogene glaciations. *Quat. Int.* 40, 43–52.
- Lourens, L., Hilgen, F.J., Gudjonsson, L., Zachariasse, W.J., 1992. Late Pliocene to early Pleistocene astronomically forced sea surface productivity and temperature variations in the Mediterranean. *Mar. Micropaleontol.* 19, 49–78.
- Mai, D.H., 1995. *Tertiäre Vegetationsgeschichte Europas*. Gustav Fischer, Jena.
- Martin, J.M., Braga, J.C., 1994. Messinian events in the Sorbas basin in southeastern Spain and their implication in the recent history of the Mediterranean. *Sediment. Geol.* 90, 257–268.
- Mayr, H.M., 1979. *Gebissmorphologische Untersuchungen an miozänen Gliriden (Mammalia, Rodentia) Süddeutschlands*. Ph.D. Thesis, University Ludwigs Maximilians, München.
- Mein, P., 1984. Composition quantitative des faunes de mammifères du Miocène moyen et supérieure de la région lyonnaise. *Paléobiol. Continentale* 14, 339–347.
- Mein, P., 1990. Updating of MN zones. In: Lindsay, E.H., Fahlbusch V., Mein, P. (Eds.), *European Neogene Mammal Chronology*. Plenum, New York, pp. 73–90.
- Mein, P., Moissenet, E., Adrover, R., 1990. Biostratigraphie du Néogène supérieur de Teruel. *Paleontol. Evoluc.* 23, 121–139.
- Mercer, J.H., 1983. Cenozoic glaciation in the Southern Hemisphere. *Ann. Rev. Earth Planet. Sci.* 11, 99–132.
- Miesch, A.T., 1976. *Q-mode factor analysis of geochemical and petrologic data matrices with constant sum rows*. U.S. Geol. Surv. Prof. Pap. 574-G, 1–47.
- Miller, K.G., Wright, J.D., Fairbanks, R.G., 1991. Unlocking the Ice House: Oligocene–Miocene oxygen isotopes, eustasy and margin erosion. *J. Geophys. Res.* 96, 6829–6848.
- Montuire, S., 1994. *Communautés de mammifères et environnements*. Ph.D. Thesis, University Montpellier II.
- Morgan, M.E., Kingston, J.D., Marino, B.D., 1994. Carbon isotopic evidence for the emergence of C4 plants in the Neogene from Pakistan and Kenya. *Nature* 367, 162–165.
- Morgan, M.E., Badgley, C., Gunnell, G.F., Gingerich, P.D., Kappelman, J.W., Maas, M.C., 1995. Comparative paleoecology of Paleogene and Neogene mammal faunas: body-size structure. *Palaeogeogr., Palaeoclimatol., Palaeoecol.* 115, 287–318.
- Mudie, P.J., Helgason, J., 1983. Palynological evidence for Miocene climatic cooling in eastern Iceland about 9.8 Myr ago. *Nature* 303, 689–692.
- Nicholson, S., Flohn, H., 1980. African environmental and climatic changes and the general circulation in late Pleistocene and Holocene. *Climatic Change* 2, 313–348.
- Niethammer, J., Krapp, F., 1978. *Handbuch der Säugetiere Europas*. Akademische Verlagsgesellschaft, Wiesbaden.
- Nowak, R.M., 1991. *Walker's Mammals of the World*. Johns Hopkins University Press, Baltimore.
- Opydyke, N., Mein, P., Moissenet, E., Pérez-Gonzalés, A., Lindsay, E., Petko, M., 1990. The magnetic stratigraphy of the Late Miocene sediments of the Cabriel Basin, Spain. In: Lindsay, E.H., Fahlbusch V., Mein, P. (Eds.), *European Neogene Mammal Chronology*. Plenum, New York, pp. 507–514.
- Oslick, J., Miller, K., Feigenson, M.D., Wright, J.D., 1994. Oligocene–Miocene strontium isotopes: Stratigraphic revisions and correlations to an inferred glacioeustatic record. *Paleoceanography* 5, 427–443.
- Perlmutter, M.A., Matthews, M.D., 1999. Global cyclostratigraphy — a model. In: Cross, T. (Ed.), *Quantitative Dynamic Stratigraphy*. Prentice Hall, Englewood Cliffs, N.J. (in press).
- Pickford, M., Morales, J., 1994. Biostratigraphy and palaeobiogeography of East Africa and the Iberian peninsula. *Palaeogeogr., Palaeoclimatol., Palaeoecol.* 112, 297–322.
- Pimm, S.L., 1978. An experimental approach to the effects of predictability on community structure. *Am. Zool.* 18, 797–808.
- Poore, R., 1981. Late Miocene biogeography and paleoclimatology of the central North Atlantic. *Mar. Micropaleontol.* 6, 599–616.
- Potts, R., Behrensmeyer, A.K., 1992. Late Cenozoic terrestrial ecosystems. In: Behrensmeyer, A.K., Damuth, J., DiMichele, W., Potts, R., Sues, H.D., Wing, S. (Eds.), *Terrestrial Ecosystems through Time*. University of Chicago Press, Chicago, pp. 419–519.
- Precht, H., Christopherson, J., Hensel, H., Larcher, W., 1973. *Temperature and Life*. Springer, Berlin.
- Putman, R.J., 1994. *Community Ecology*. Chapman and Hall, London.
- Quade, J.T., Cerling, T.E., 1995. Expansion of C4 grasses in the Late Miocene of Northern Pakistan: evidence from stable isotopes in paleosols. *Palaeogeogr., Palaeoclimatol., Palaeoecol.* 115, 91–116.
- Quade, J.T., Cerling, T.E., Bowman, J.R., 1989. Development of the Asian monsoon revealed by marked ecological shift in the latest Miocene of northern Pakistan. *Nature* 342, 163–166.
- Quade, J.T., Solounias, N., Cerling, T.E., 1994. Stable isotope evidence from paleosol carbonates and fossil teeth in Greece for forest or woodlands over the past 11 Ma. *Palaeogeogr., Palaeoclimatol., Palaeoecol.* 108, 41–53.
- Renner, R.M., 1993. The resolution of a compositional dataset

- into mixtures of fixed source compositions. *Appl. Stat.* 42, 615–631.
- Reumer, J.W.F., 1994. Phylogeny and distribution of the Crocidoriscinae (Mammalia; Soricidae). *Carnegie Mus. Nat. Hist. Spec. Publ.* 18, 345–356.
- Reyment, R.A., Jöreskog, K.G., 1993. *Applied Factor Analysis in the Natural Sciences*. Cambridge University Press, Cambridge.
- Robin, G. de Q., 1988. The Atlantic ice sheet: its history and response to sea level and climatic changes over the past 100 million years. *Palaeogeogr., Palaeoclimatol., Palaeoecol.* 67, 31–50.
- Ruddiman, W.F., McIntyre, A., 1984. Ice-thermal response and climate role of the surface Atlantic Ocean: 40°N to 63°N. *Geol. Soc. Am. Bull.* 95, 381–396.
- Schaeffer, R., Spiegler, D., 1986. Neogene Kälteeinbrüche und Vereisungsphasen im Nordatlantik. *Z. Dtsch. Geol. Ges.* 137, 537–552.
- Schaub, S., 1938. Tertiäre und Quartäre Murinae. *Abh. Schweiz. Paläontol. Ges.* 61, 1–39.
- Schwarzbach, M., 1968. Das Klima des rheinischen Tertiärs. *Z. Dtsch. Geol. Ges.* 118, 33–88.
- Sierro, F.J., Flores, J.A., Civis, J., Gonzáles Delgado, J.A., Francés, G., 1993. Late Miocene globorotaliid event-stratigraphy and biogeography in the NE-Atlantic and Mediterranean. *Mar. Micropaleontol.* 21, 143–168.
- Simberloff, D., Dayan, T., 1991. The guild concept and the structure of ecological communities. *Annu. Rev. Ecol. Syst.* 22, 115–143.
- Slobodkin, L.B., Sanders, H.L., 1969. On the contribution of environmental predictability to species diversity. *Brookhaven Symp. Biol.* 22, 82–95.
- Storch, G., 1978. Familie Gliridae Thomas 1897 — Schläfer. In: Niethammer, J., Krapp, F. (Eds.), *Handbuch der Säugetiere Europas*. Akademische Verlagsgesellschaft, Wiesbaden, pp. 201–279.
- Storch, G., Zazhigin, V.S., 1996. Taxonomy and phylogeny of the *Paranourosorex* lineage: Neogene of Eurasia (Mammalia: Soricidae: Anourosoricini). *Paläontol. Z.* 70, 257–268.
- Storch, G., Engesser, B., Wuttke, M., 1996. Oldest fossil record of gliding in rodents. *Nature* 379, 439–441.
- Tallis, J.H., 1991. *Plant Community History*. Chapman and Hall, London.
- ter Braak, C.F.J., 1986. Canonical correspondence analysis: a new eigenvector technique for multivariate direct gradient analysis. *Ecology* 67, 1167–1179.
- ter Braak, C.F.J., 1987. The analysis of vegetation–environment relationships by canonical correspondence analysis. *Vegetation* 69, 69–77.
- Van Couvering, J.A.H., 1980. Community evolution in Africa during the Late Cenozoic. In: Behrensmeyer, A.K., Hill, A.P. (Eds.), *Fossils in the Making*. University of Chicago Press, Chicago, pp. 272–298.
- van Dam, J.A., 1996. Stephanodonty in fossil murids: a landmark-based morphometric approach. In: Marcus, L.F., Corti, M., Loy, A., Naylor, G.J.P., Slice, D.E. (Eds.), *Advances in Morphometrics*. NATO volume 284, Plenum, New York, pp. 449–461.
- van Dam, J.A., 1997. The small mammals from the upper Miocene of the Teruel–Alfambra region (Spain): paleobiology and paleoclimatic reconstructions. *Geol. Ultraiectina* 156, 1–204.
- van der Meulen, A.J., Daams, R., 1992. Evolution of Early–Middle Miocene rodent faunas in relation to long-term palaeoenvironmental changes. *Palaeogeogr., Palaeoclimatol., Palaeoecol.* 93, 227–253.
- van der Meulen, A.J., de Bruijn, H., 1982. The mammals from the Lower Miocene of Aliveri (Island of Evia, Greece), Part 2. The Gliridae. *Proc. K. Ned. Acad. Wet. B* 85, 485–524.
- van der Zwaan, G.J., Gudjonsson, L., 1986. Middle Miocene–Pliocene stable isotope stratigraphy and paleoceanography of the Mediterranean. *Mar. Micropaleontol.* 10, 71–90.
- van de Weerd, A., 1976. Rodent faunas of the Mio–Pliocene continental sediments of the Teruel–Alfambra region: Spain. *Utrecht Micropaleontol. Bull. Spec. Publ.* 2, 1–217.
- Van Valen, L., 1964. Relative abundance of species in some fossil mammal faunas. *Am. Nat.* 93, 109–116.
- Vincent, E., Killingley, S., Berger, W.H., 1980. The Magnetic Epoch 6 carbon shift: a change in the ocean's $^{13}\text{C}/^{12}\text{C}$ ratio 6.2 million years ago. *Mar. Micropaleontol.* 5, 185–203.
- Weltje, G.J., 1994. Provenance and dispersal of sand-sized sediments. *Geol. Ultraiectina* 121, 1–208.
- Weltje, G.J., 1997. End-member modelling of compositional data: Numerical–statistical algorithms for solving the explicit mixing problem. *J. Math. Geol.* 29, 503–547.
- Wing, S.L., Sues, H.D., Potts, R., DiMichele, W., Behrensmeyer, A.K., 1992. Evolutionary Paleoecology. In: Behrensmeyer, A.K., Damuth, J., DiMichele, W., Potts, R., Sues, H.D., Wing, S. (Eds.), *Terrestrial Ecosystems through Time*. University of Chicago Press, Ill., pp. 1–13.
- Wolfe, J.A., 1985. Distribution of major vegetational types during the Tertiary. *Am. Geophys. Union, Geophys. Monogr.* 32, 357–375.
- Wolfe, J.A., 1994. An analysis of Neogene climates in Beringia. *Palaeogeogr., Palaeoclimatol., Palaeoecol.* 108, 207–216.
- Wolf-Welling, T.C.W., Winkler, A., O'Connell, S., Cremer, M., Rack, F., Statterger, K., Thiede, J., 1995. Northern Hemisphere cooling starting at 10.5 Ma: coarse fraction analysis of Fram Strait Sites 908 and 909 (Leg 151 NAAG). Abstract for congress, *Prediction in Geology*, Amsterdam.
- Wright, J.D., Miller, K.G., 1992. Miocene stable isotope stratigraphy Site 747: Kerguelen Plateau. *Proc. ODP, Sci. Results* 120, 855–866.
- Wright, J.D., Miller, K.G., Fairbanks, R.G., 1991. Evolution of modern deepwater circulation: evidence from the late Miocene Southern Ocean. *Paleoceanography* 6, 275–290.